Chapter 1

Introduction

1.1 Preface

Since industry revolution, there are a lot of discoveries and technologies which bring great, deep and far impact on the human civilization. In particular, the electronic display technology goes deep into many fields in human daily life. Its widespread applications, such as entertainment, education and communication, motivate people to develop more powerful and comfortable display technologies.

For the electronic display technology, there are a few milestones in past 120 years as shown in Fig. 1.1 [1]. In 1897, K. F. Braun invented the cathode ray tube (CRT) which gave birth to the following various kinds of CRT monitors and TV. The widespread success of the CRT as an information display opened the door for the development of flat panel display technology such as liquid crystal displays (LCDs) and plasma display panels (PDPs). They are getting more and more popular after 1990s because they provide comparable image quality with CRT but have compact sizes and low power consumption.

Over the past century, people made huge progress in better image qualities and more compact instruments, i.e. from black-and-white to color types and bulky to compact sizes. Various scenes and information are reproduced and spread by the electronic displays. However, so far as the image qualities are concerned, they are still not as good as the real vision perceived by human eyes in the real world. The display performances of the above-mentioned technologies are limited by only one viewpoint of the objects is provided. In other words, there is no stereoscopic sense included in

the display images. This kind of display technologies are classified as 2D display.

For some important applications which require higher spatial resolution, such as the military flying training and distance medical treatment, the image qualities of conventional 2D display seem more and more insufficient. Therefore, to pursue for more natural viewing and practical needs, 3D display technology is expected to be the next key display technology and shall play an important role in the future.

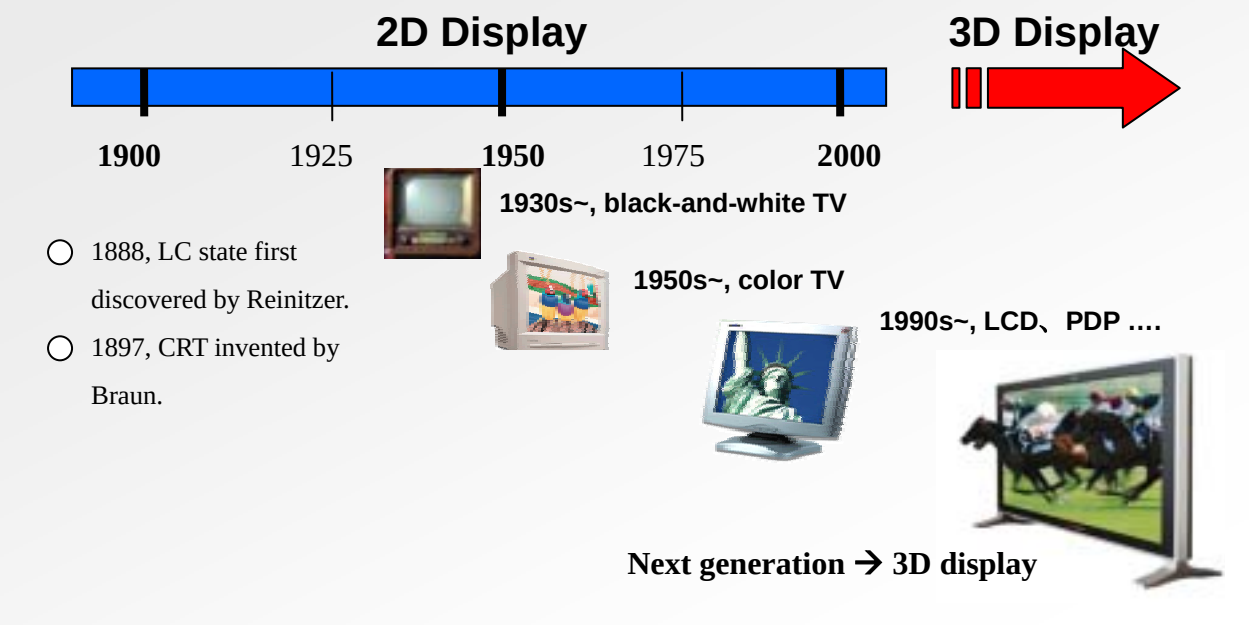

Fig. 1.1 Historical development of the electronic displays

1.2 Principle of 3D Vision

Before the introduction to various kinds of 3D display technology, some results of the researches on visual science must be discussed and learned first. Three-dimensional information obtained by the visual system is processed by complex activities in the brain. A lot of related researches have been made in this field [2]. There are several clues to depth perception by the visual sense as shown in Fig. 1.2, and which clue will be dominant depends on depth distance [3,4].

Convergence

Convergence as a depth clue is very effective when the distance is small, and is considered to be effective for up to 20 m. Convergence rapidly loses its effects as the distance increases (because the convergence angle gets smaller).

Binocular parallax

Binocular parallax occurs when there are other objects in front of or behind the object on which the right-left eyes are focused. If the degree of this binocular parallax is sufficiently small, the images are fused and the observer has a clear sensation of depth before and after the object. The binocular parallax is effective and precise in recognizing the depth difference, i.e. the difference in the distance between several objects. It is an important factor in understanding the relative position of objects in 10 m.

Accommodation and Motion Parallax

Accommodation is only effective when the observation distance is no more than 2 to 3 m. Depth perception brought about by motion parallax also provides an important clue as to depth, and can be as effective as binocular parallax under certain conditions.

Others

As effects such as linear perspective, light and shade, overlapping and aerial perspective can be easily achieved in actually shot 2D images, they are not list in Fig. 1.2.

Some of those clues list in Fig. 1.2 are especially important for the capabilities of 3D display. Primary research targets in 3D image technology are binocular parallax, accommodation, convergence, and motion parallax (or look-around capability: changes of viewpoint accompanied with head movement). When displaying a stereoscopic image, the characteristics that may be trade-off frequently are also shown at the bottom of Fig. 1.2.

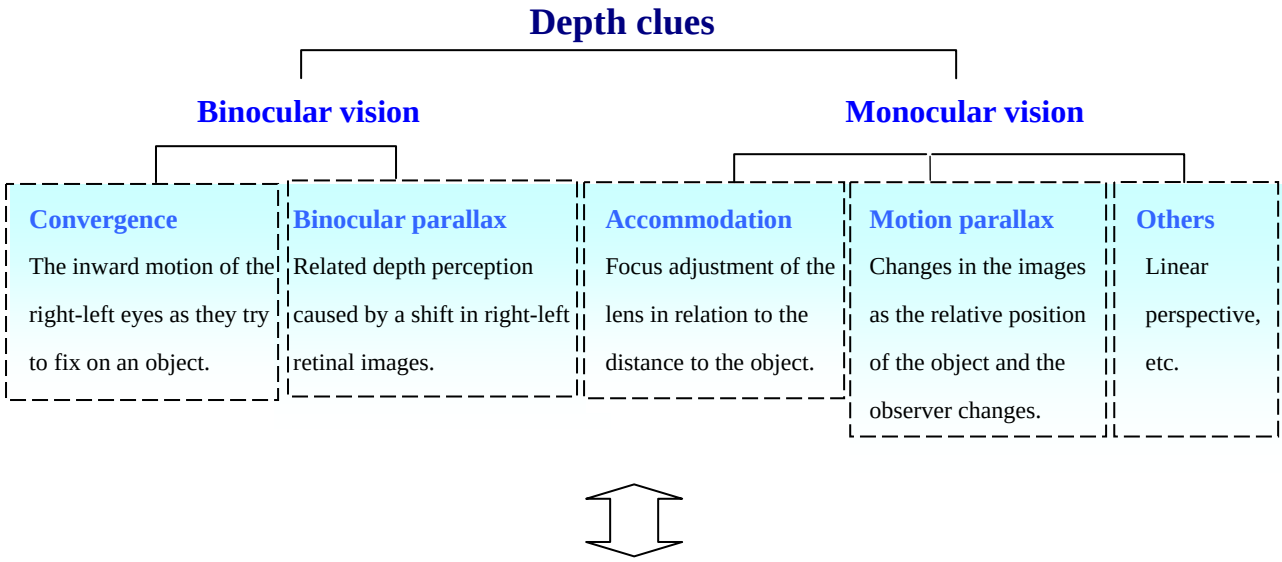

Restriction of actual display

Limitation of :

- screen size (size of viewing angle) and viewing distance
- stereo viewing area (3D range of direction against the screen)
- picture quality (brightness, resolution, field/frame rate, etc.

Usage of special equipment:

- special glasses, sensors for head-tracking, etc.

Fig. 1.2 Depth clues and display factors

Visual information received through one eye is not the same as that through the other eye, but we perceive these data as a single image. This ability, i.e. binocular vision, appears to be based on interaction of the right and left images, and this ability is an important function in the design of a 3D display. In addition, the average distance between the pupils of the human eyes is approximately 65 mm which is adopted commonly when considering the viewing condition.

1.3 Introduction to 3D Display Technology

The history of 3D display goes back to the early 1800s. Early devices include the Wheatstone stereoscope and the Brewster stereoscope [5]. However, most practical 3D techniques are developed after the middle period of 20th century.

Generally speaking, the 3D Display can be divided into two types: **stereoscopic displays** and **auto-stereoscopic displays** according to the usage of special apparatus.

Stereoscopic displays require users to wear a device, such as polarized glasses, that ensures the left and right views are seen by the correct eye. Many stereoscopic display designs have been proposed and there are reviews of these in several sources [6,7]. Most of them are mature systems and have become established in several professional markets but suffer the drawback that the viewer have to wear, or be very close to, some devices to separate the left and right views. This limited the widespread appeal of stereoscopic systems as personal displays for home and office use even when 3D effect is appealing.

Auto-stereoscopic displays are those that do not require the observer to wear any device to separate the left and right views and instead send them directly to the correct eye. This removes a key barrier to the acceptance of 3D display for everyday use but requires a significant change in 3D display design. This subject is discussed in the following.

1.3.1 Methods of Generating Sense of Depth

For auto-stereoscopic displays, various methods have been proposed up to present. The methods of generating sense of depth can be roughly categorized into three types and each includes a few minor items respectively [8]. They are listed in the following.

Volumetric type

(a) drawing 3D profiles on a scattering medium with a scattering laser beam [9], as shown in Fig. 1.3(a).

(b) projecting or scanning layered images on a spatially designed screen to create a volumetric image profile [10,11], as shown in Fig. 1.3(b).

(c) inducing psychological effects with use of a super-large image projection screen [12], as shown in Fig. 1.3(c).

Holographic type

(d) displaying interference fringes generated by the superposition of rays from each object point [13], as shown in Fig. 1.3(d).

Stereo pair type

(e) presenting a spatial [14,15,16] or a time [17] multiplexed sequence of many different viewing images with a viewing zone forming optics, as shown in Fig. 1.3(e).

In short, there are two ways to generate the sense of depth. The first one is to simulate the situation that objects exist in the real space, as suggested by methods (a) to (d). The second is to directly send pairs of parallax images to each eye respectively, as suggested by method (e). The major types are named after their featured principles, i.e. spatial characteristics, holography, and stereo pair, respectively.

1.3.2 Comparisons between Various 3D Methods

Each 3D method has some advantages and disadvantages. Table 1.1 lists their comparisons according to the 3D image qualities, system size and price [18]. The major drawback of stereoscopic display is undesirable supplementary devices are required. On the other hand, the volumetric type often has bulky appearances and

Method (a)

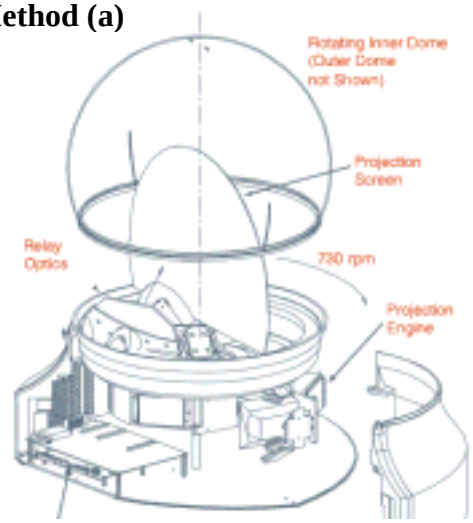

"Volumetric 3D Display System with Rasterization Hardware," *Stereoscopic Displays and Virtual Reality Systems VIII*, Proc. of SPIE (2001).

Method (b)

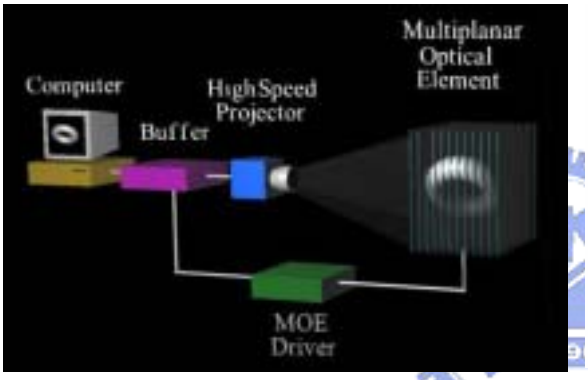

"A Solid-state Multi-planar Volumetric Display", SID (2003)

Method (c)

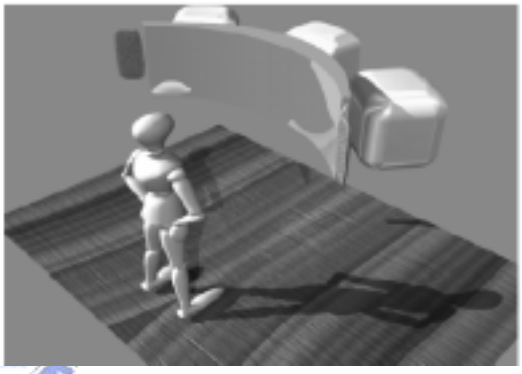

"DSHARP –A Wide Screen Multi-projector Display", SID (2003)

Method (d)

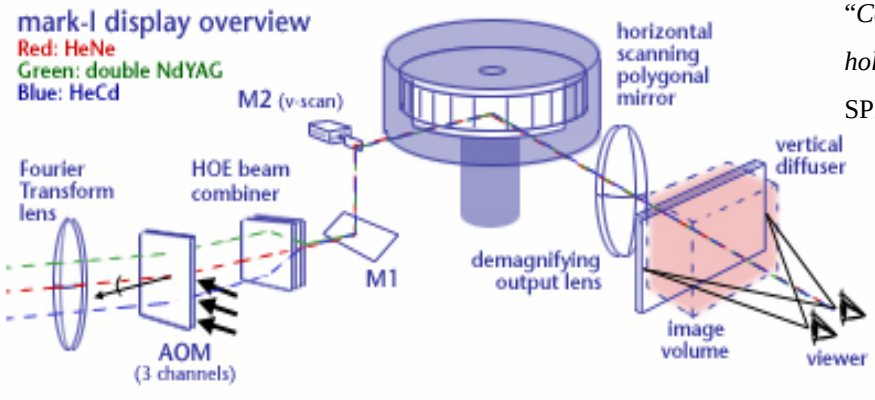

"*Color images with the MIT holographic video display*", SPIE (1992).

Fig. 1.3 Examples of 3D methods: (a) volumetric 3D display system with rasterization hardware [9]; (b) a solid-state multi-planar volumetric display [10]; (c) DSHARP – a wide screen multi-projector display [12]; (d) color images with the MIT holographic video display [13]

Method (e)

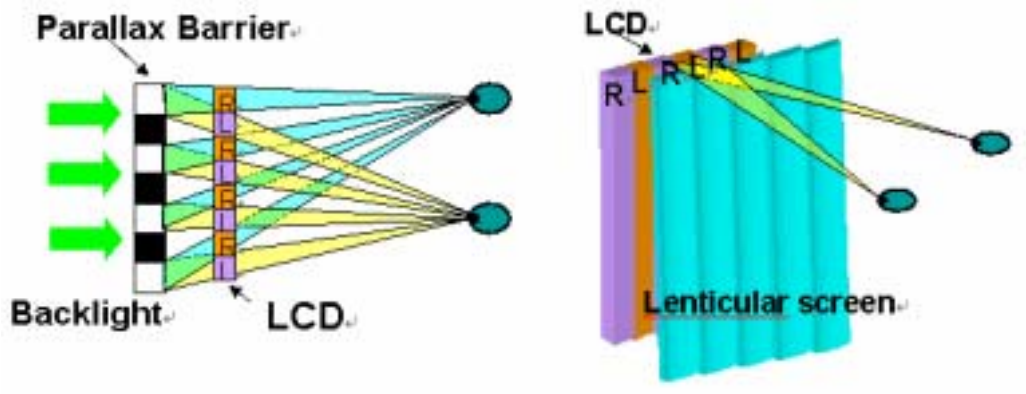

Fig. 1.3 Examples of 3D methods: (e) stereo pair type (contd.)

limited 3D effect, such as poor reproduction in solid objects. Again, the holographic type has poor feasibility due to the requirement of ultrahigh technical support. Among these, the overall appreciations of the stereo pair type are best. It not only has high feasibility but also has compatibility with the current 2D display technology. Besides, the image qualities are not sacrificed. That is why the stereo pair type is applied in most of the available auto-stereoscopic displays today, and deserves more attentions here.

Table 1.1 Comparisons between various 3D displays

	Stereoscopic	**Auto-stereoscopic**		
		Volumetric	**Holographic**	**Stereo pair**
Natural depth	メ-△	メ-△	△-○	△-○
Viewer comfort	メ	メ-△	△-○	△-○
Group viewing	○	○	○	△-○
Compatibility: 2D/3D	○	△-○	メ-△	○
No degrade image quality	○	△-○	△	○
Compact size	○	メ-△	メ	△-○
Moderate price	○	メ-△	メ	○

○: Possible　△: Some cases possible　メ: Impossible

1.3.3 Stereo Pair Type

According to the image presentation methods, the stereo pair type can also be divided into two types: **time-parallel** (or spatial-multiplexed) and **time-multiplexed types**. As implied by the name, the time-parallel type displays the stereo pairs at the same time and the time-multiplexed type displays the stereo pairs sequentially, as shown in Fig.1.4.

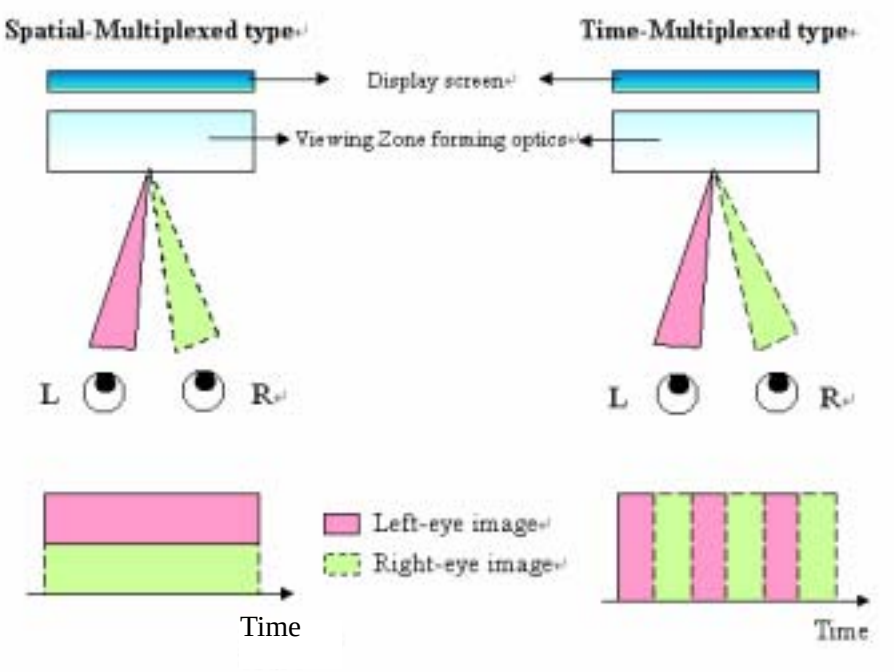

Fig. 1.4 Principles of the spatial-multiplexed and time-multiplexed types

Both of them require viewing zone forming optics to send the parallax images to each correct eye. The viewing zone is a spatial location where the viewers can see the entire images displayed on the screen. Two viewing zones, one for one eye and another for another eye, form a complete 3D vision. To do this, each imaging system needs an optical plate with a specific optical power.

As for the time-parallel method, a lenticular screen, a parallax barrier and a micro-lens array plate like IP (integral photography) are well-known examples, as shown in Fig. 1.3 (contd.) and Fig. 1.5 [19,20]. These plates are usually combined

with flat panel devices and separate different view images. However, these plates reveal some undesirable characteristics. The pixels on the panel are often divided into regions for different image information and the resolution of each eye image is reduced into one half or less. Besides, the lenticular screen and parallax barrier have limited image clarity and viewing zone uniformity. Moreover, the parallax barrier lowers the image brightness. The micro-lens array plate has so far no standard form of manufacture and has a limited resolution.

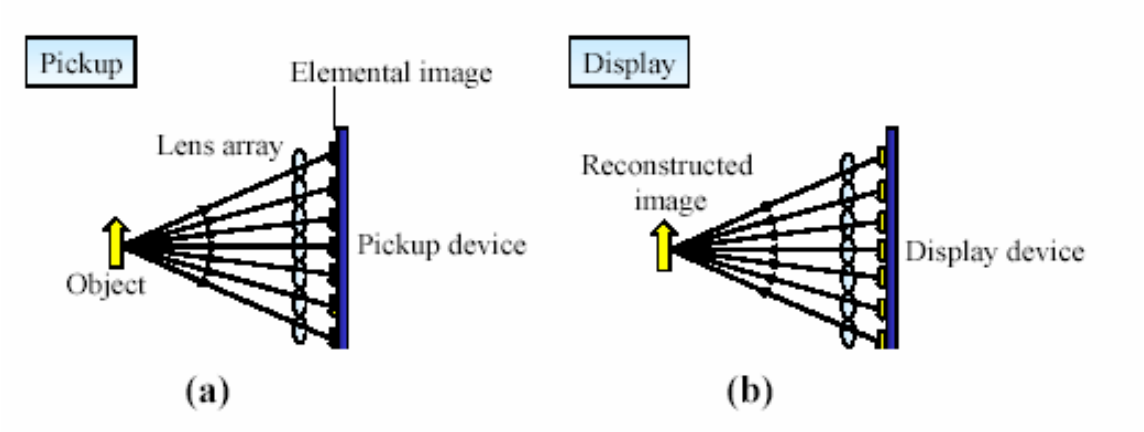

Fig. 1.5 Concept of integral imaging: (1) pick up (b) display

As for the time-multiplexed method, its development was hindered in early days because the displays of fast response time were not available then. In 2001, a 3D display using field-sequential LCD with light direction controlling back-light was disclosed [21], as shown in Fig. 1.6. Its viewing zones were formed by a lenticular screen and a LC shutter. By switching the LC shutter, the lights for left and right eyes are separated in desired directions. Another example was proposed by Mitsubishi in 2003 [22]. Its viewing zone forming optics consists of a light-guide plate and a double-sided prism sheet, as shown in Fig. 1.7. After emitted from bottom light-guide, light penetrates into the double-sided prism sheet and is reflected to the certain direction due to TIR. By switching two light sources sequentially, pairs of parallax images are perceived by each eye and thus form the 3D vision. In 2004, another

similar design for time-multiplexed 3D display was proposed by K. W. Chien [23], as shown in Fig. 1.8.

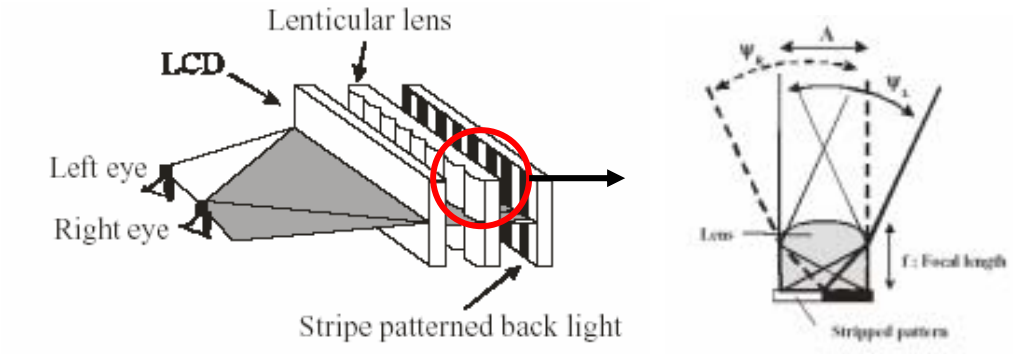

Fig. 1.6 A 3D display using field-sequential LCD with light direction controlling backlight (2001) [21]

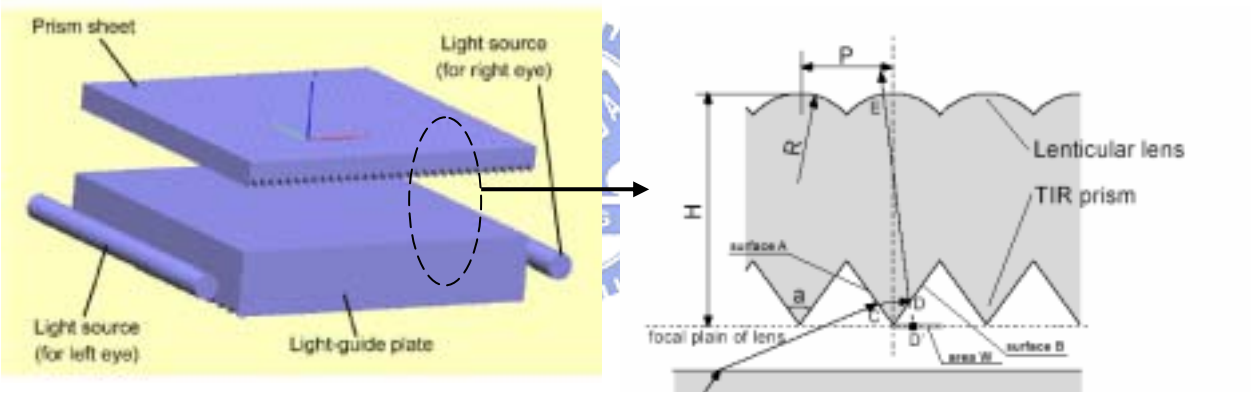

Fig. 1.7 Dual directional backlight for stereoscopic LCD (2003) [22]

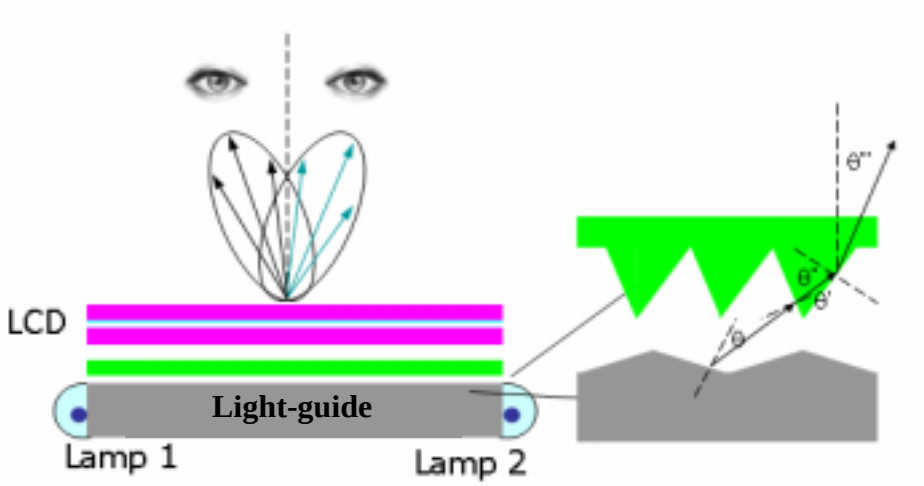

Fig. 1.8 3D mobile display based on sequentially switching backlight with focusing foil [23]

The common feature of the time-multiplexed 3D display is the resolution is the same as that of the LCD used, which is not feasible in time-parallel method. However, the viewing zones forming optics of the well-known designs based on the time-parallel method were complex and had some drawbacks. Misalignment between the lenticular screen and LC shutter in first design, or patterns on the double-sided prism sheet in the second design, resulted in the shift of viewing zones. Besides, the light efficiency was reduced in the first design due to the blocking of the LC shutter. In last two designs, inadequate light efficiency resulted from the bottom light-guide which was too flat to guide light effectively.

1.3.4 Summary

Various 3D display technologies have been discussed above. Many of them can provide not bad 3D images but very few can perform more than one satisfactory function, except stereo pair type. Compared with other 3D display technologies, the stereo pair type has many advantages, such as good image qualities, compact size, high feasibility, and compatibility with current 2D display technology.

Among various kinds of the stereo pair type, the time-multiplexed method has an inherent advantage of no needs to sacrifice spatial qualities for displaying different image information. It further implies no alignment issue between the displayed images and the viewing zone forming optics and thus reduces crosstalk factors.

As a result, the benefits of the time-multiplexed method based on stereo pair type will attract more researches involved in the future if enough supports come from various peripheral technologies.

1.4 Motivation and Objective of this Thesis

To pursue for more natural viewing and practical needs, as discussed above, 3D display technology is expected to be the next key display technology and shall play the leading role in the future. Among them, the time-multiplexed method of stereo pair type is superior due to the compatibility with current flat panel display technology and the compatible image qualities with 2D display. The only issue is, just like other auto-stereoscopic displays, it can not provide group viewing of high qualities. From another viewpoint, however, it is the unique candidate for the 3D mobile display.

In the past few years, several articles have been devoted to such topic, as mentioned above. A complete time-multiplexed 3D display based on stereo pair type consist of three parts, including driving circuits, fast switching LC panel and directional backlight. Each part can be isolated as an independent research topic. Especially, the requirements and developments of the first two parts are similar to those of the flat panel TVs, which have been actively studied in related fields. Here, we only consider the directional backlight. The known designs, as mentioned above, have complex backlight structures, i.e. more than two micro patterns are needed, and some drawbacks, such as alignment issue and inadequate light efficiency.

. As a result, the objective of this thesis is to propose a novel dual directional backlight for 3D mobile display based on time-multiplexed stereo pair type. This dual directional backlight system has the benefits of simpler structures and no alignment issue. The characteristic of this design is to make use of two identical light-guides, each patterned with micro-groove structures on one surface, to direct light into the left-eye and right-eye directions, respectively.

1.5 Organization of this Thesis

The thesis is organized as following: The principle and design of the dual directional Backlight is presented in **Chapter 2**. In **Chapter 3**, the technology to fabricate the directional light-guide is introduced, and the major instruments used to characterize the directional light-guide are also described. The simulated results are presented in **Chapter 4**. The experimental results, including the fabricated directional light-guide, dual directional backlight, and the evaluated results, will be in **Chapter 5**. Finally, the applications of the proposed dual directional backlight and the conclusions of this thesis will be presented in **Chapter 6** and **Chapter 7**, respectively.

Chapter 2

Design of Dual Directional Backlight System

2.1 Introduction

A directional light-guide with light-controlled ability of one direction was proposed and designed in this chapter. A plurality of micro-groove structures is patterned on one surface of the light-guide to redirect the light into the desired directions due to TIR. With combining two identical directional light-guides, a dual directional backlight is formed and thus can be applied for time-multiplexed 3D display. In addition, some solutions were proposed to suppress the moiré` pattern which might occur when two periodic structures were superimposed.

2.2 Design of Directional Light-guide

After choosing the time-multiplexed method of stereo pair type for the design target, next step is to design a proper viewing zone forming optics which sends light into right-eye and left-eye, respectively. Among the common light-controlled optics, such as reflective, refractive, and diffractive optics, the reflective optics has the advantage of high light efficiency and is easy to be controlled and predicted. However, it needs extra work to make the light-controlled pattern with reflective characteristic. Therefore, the total internal reflection (TIR) seems to be a good choice and a directional light-guide based on it is proposed and discussed in detail in the following.

In this directional light-guide, simple micro-grooved structures are patterned on one surface of the light-guide to control the light direction, as shown in Fig. 2.1(a). The light source is set on the side which faces the inclined surface of the

micro-groove. After light enters the light-guide, all light is trapped in the light-guide due to TIR, until being coupled out by the grooves or penetrating the opposite side. Since the emitted light of light source centralizes in the horizontal direction, most light are totally internal reflected by the micro-grooves and finally redirected to the desired direction. The relationship between incident and emerging angle of ray can be calculated by Snell` s Law, as shown in Fig. 2.1(b). In this way, one light-guide has the light-controlled ability of one direction. In order to provide a uniform

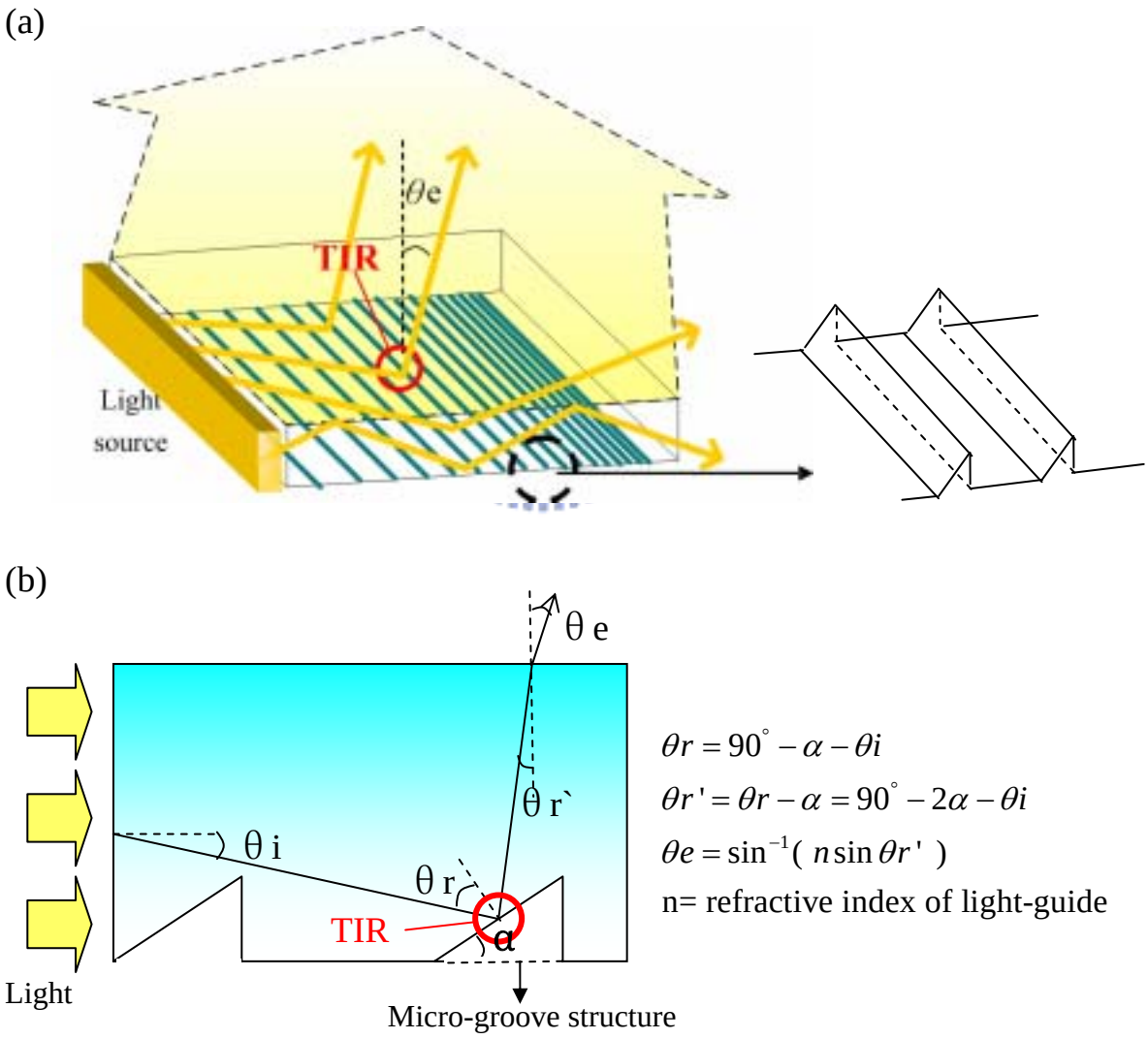

Fig. 2.1 (a) Micro-groove structures on the light-guide and (b) relationship between each angle

image to the certain viewing direction, the structure and distribution of the micro grooves need to be further considered as following.

2.2.1 Inclined Angle of Micro-groove Structure, α

The first key point is to control the light into the desired direction. In this design, TIR at the grooves is required to redirect the light into the desired direction and hence should be guaranteed. Here, we assume the material of light-guide is PMMA (n=1.49) and discuss how light interacts with the micro-groove structures in detail.

For convenience, we assume that most incident rays concentrate around the horizontal direction and thus the incident ray of zero degree ($\theta i = 0$) can be an object for discussion. Table 2.1 lists each angle value under different inclined angle of micro-groove structure (α), which are calculated from the formulas listed in Fig. 2.1(b). If α is too small (< 23.5°), most light is still trapped in the light-guide due to the TIR on the top surface of light-guide. If α is too large (> 48°), most light penetrate the micro-groove pattern directly and cannot be totally internal reflected to the desired direction. As a result, for the incident ray of zero degree, a functioning range of α for TIR on micro-groove surfaces is located between 23.5° and 48°.

Following the assumption above, the incident rays of nonzero degree are further taken into consideration, as shown in Fig. 2.2. For the incident ray of incident angle of smaller than ($48^\circ - \alpha$), TIR at the grooves still occurs because the interlaced angle between the incident ray and the normal of the micro-groove inclined surface is larger than the critical angle. If the incident angle is larger than ($48^\circ - \alpha$), the incident ray will penetrate the grooves directly or being coupled out of the light-guide in a large angle due to TIR at the grooves. As the incident ray penetrates the grooves, about 4% reflection on the inclined groove surfaces follows from the Fresnel equations with the

refractive index of PMMA equal to 1.49[24] .

After light enters the light-guide, in short, most of the light is emitted in a certain angular range to form a viewing cone for one of the viewer` s eyes except little light leakage in the opposite direction. In addition to the consideration above, the accurate inclined angle value further depends on the simulated results and performance requirements, which will be discussed more clearly in chap. 4.

Table 2.1 $\theta i = 0$, each angle value under different inclined angle of micro-groove structure (α) * n=1.49 , $\theta c \sim 42^\circ$

α (degree)	θr (degree)	$\theta r'$ (degree)	θe (degree)
< 23.5	> 66.5	> 43	TIR on top surface of light-guide
30	60	30	~48
35	55	20	~30.5
40	50	10	~15
45	45	0	0
> 48	< 42	No TIR happens on the inclined surface of micro-groove structure	

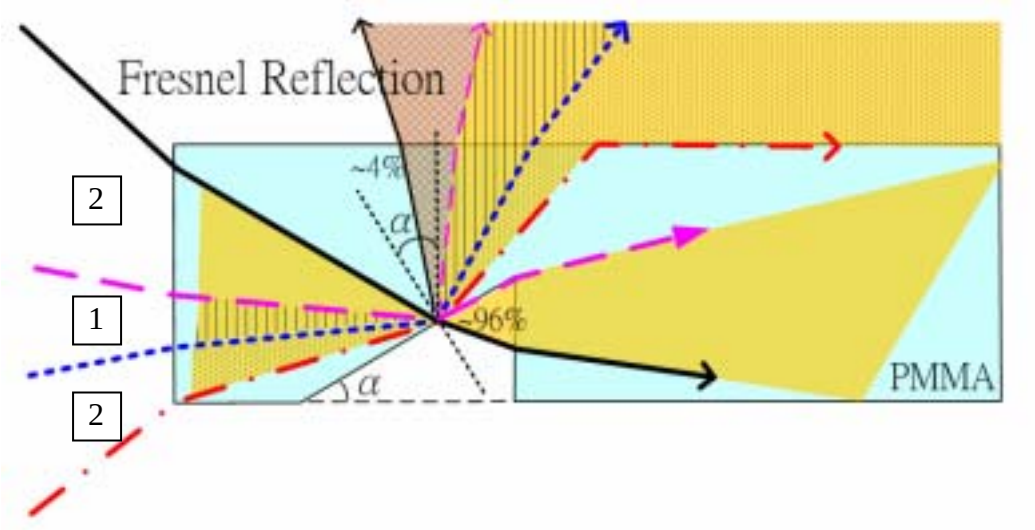

Fig. 2.2 Possible light paths for the incident rays of nonzero degree: (1) incident angle smaller than ($48^\circ - \alpha$); (2) incident angle larger than ($48^\circ - \alpha$)

2.2.2 Distribution of Micro-groove Structures

Another key point is to provide a uniform image which is determined by the uniformity of light on the top surface of light-guide. As further away from the light source, the light intensity decreases. In order to couple out light uniformly, the groove density is higher as the groove is further away from the light source. In application, the groove density can be adjusted by the pattern pitch, including varying groove width or the distance between each groove or both.

2.3 Combinations of the Dual Directional Backlight System

Dual directionalities were obtained by utilizing two light source and two directional light-guide mentioned above. Due to the asymmetry of micro-groove structures, there are four possible constitutions of dual directionalities, including face-to-back, face-to-face, back-to-back and back-to-face types as plotted in Fig. 2.3. The corresponding major light paths of each light source are also shown in each plot. Each of the last three constitutions required an extra reflector to reflect light back to the desired direction. In general, the light path of light source 2(L2) is longer and more complex than that of light source 1(L1) due to its lower position. Besides, the light path with an extra reflection by the bottom reflector is also longer and more complex than that with TIR only.

Based on the principles described above, the face-to-back type is the one with simpler and shorter light paths which implies simpler light angular distribution and higher light efficiency. In practice, however, there is always a flat surface, which belongs to the package or something else, just located behind the backlight system. Its surface property, reflective or scattering, may affect the backlight performance. This concern can be removed directly by adding an extra absorber below the face-to-back

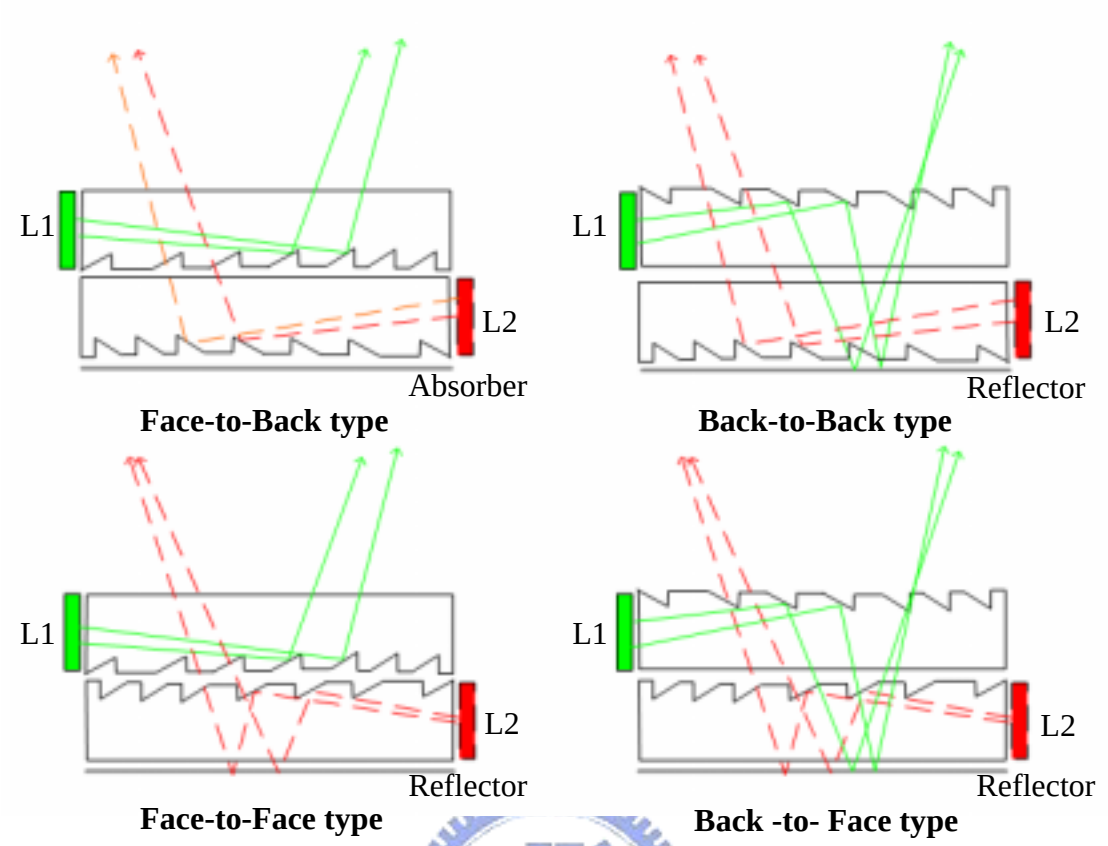

Fig. 2.3 Possible constitutions of dual directional backlight

type system. The absorber also has the advantage of preventing the unexpected and undesirable light back to the backlight system. Thus, the light leaked to the other directions was reduced.

Therefore, the face-to-back type with an absorber is taken as the composition of the dual directional Backlight in simulation and measurement. Besides, in order to match the fast switching LC panel and provide images without flickers, two light bars of LEDs were chosen as the light sources due to its fast response time, i.e. a few micro seconds.

2.4 Moire` Pattern

Furthermore, the moire` pattern, which might occur when the micro-groove structures and periodic pixels of a color filter or two micro-groove structures are

superimposed, was also considered. Because the pitch of the micro-groove structure was varied gradually on the light-guide to keep the light uniformity, it was less periodic than that of color filter. Thus, the moire` pattern generated by the first two was more serious than that generated by the last two. Besides, the moire` pattern generated by the first two was more obvious due to its closer distance to the viewer. Therefore, a few solutions were proposed to suppress the moiré` pattern generated by the color filter and the dual directional backlight. The moiré` pattern generated by the two micro-groove structures may be suppressed, too.

The first solution is to discrete the micro-groove structures into pieces as shown in Fig. 2.4(a). This method breaks the periodic characteristic of the micro-groove structures and thus suppresses the moiré` pattern effectively. The only issue is such fabrication process is hard to be acquired. The second solution is to dispose a diffuser sheet of low Haze on the top of the dual directional light-guide as shown in Fig. 2.4(b). A diffuser sheet of low Haze, about 30 %, would blur the moiré` pattern and enhance the light uniformity without damaging the light distribution. The last solution is

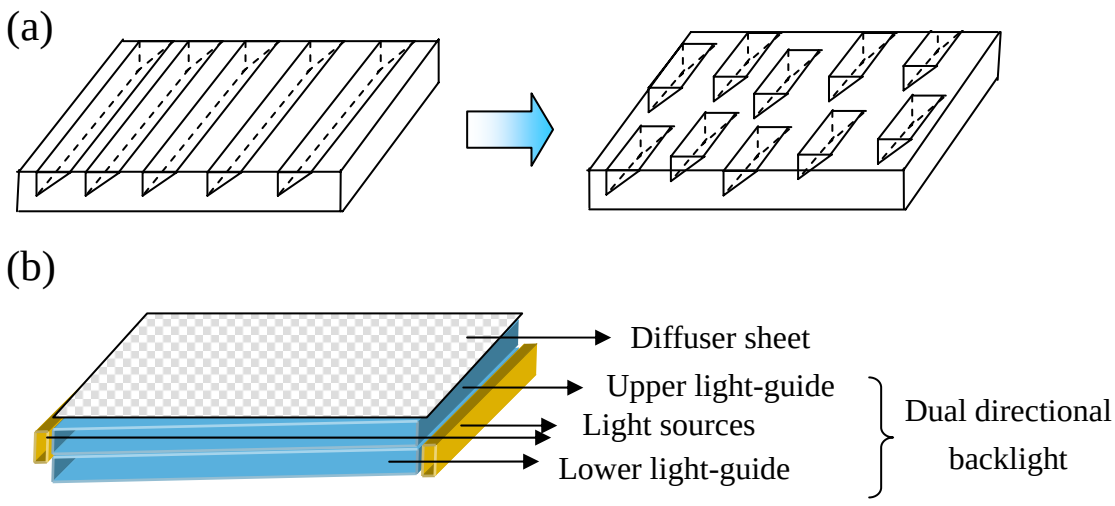

Fig. 2.4 Methods to suppress the moiré` pattern: (a) discrete groove patterns; (b) adding a diffuser sheet of low haze on the top of the backlight

to redesign the pitch ratio of the micro-groove structures and the color filter, which was described below.

A simple moiré pattern can be calculated by the following equations [25]:

$$q_1 = f_2 / f_1 \tag{2- 1}$$

$$\begin{pmatrix} f_u \\ f_v \end{pmatrix}_{k_1,k_2} = \begin{pmatrix} \cos\alpha & -\sin\alpha \\ \sin\alpha & \cos\alpha \end{pmatrix} \begin{pmatrix} k_1 \\ 0 \end{pmatrix} f_1 + \begin{pmatrix} k_2 \\ 0 \end{pmatrix} q_1 f_1, \tag{2- 2}$$

, where f_2 and f_1 are the frequencies of the periodic patterns on the color filter and the directional light-guide, respectively. The vector (f_u, f_v) denotes the spatial frequency of the moiré pattern. The angle α is the angle intercepted by the two structures, and (k_1, k_2) are the harmonic terms of each frequency. Thus, the spatial frequency f_{k_1,k_2} and the period T_{k_1,k_2} at which the moiré pattern occurs are given by the sum vector f:

$$f_{k_1,k_2} = \sqrt{{f_u}_{k_1,k_2}^{\ 2} + {f_v}_{k_1,k_2}^{\ 2}} \tag{2- 3}$$

$$T_{k_1,k_2} = \frac{1}{f_{k_1,k_2}} \quad . \tag{2- 4}$$

In order not to affect the angular distribution of the emitted light from the dual directional backlight, the angle intercepted by the two structures should be zero ideally. In this case, the period of moiré pattern under various pitch ratios of two structures was shown in Fig. 2.5. Obviously, the maximum spatial frequency of the moiré` pattern occurs when the pitch ratio is closer to 1 or 2. Therefore, the pitch ratio of micro-groove structures and the color filter must exclude such values to prevent serious moiré` pattern.

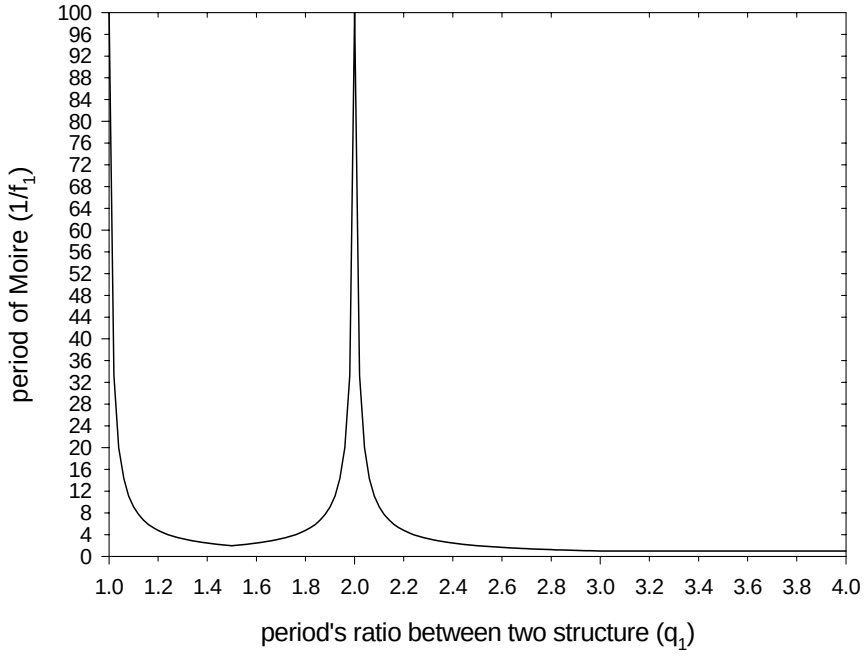

Fig. 2.4 Period of moiré pattern under various pitch ratios of two overlapped structures

2.5 Summary

A directional light-guide with one surface patterned with micro-groove structures was proposed. A dual directional backlight system which utilized two directional light-guide and two light sources was further proposed. Compared with other directional backlights mentioned in Chap 1, the proposed backlight system is simpler and easier to be fabricated without alignment issue. Besides, this backlight system has adequate light efficiency because most light is coupled out of the light-guide by the grooves, not penetrates light-guide directly.

In Chap 4, the simulation software, ASAP, will be utilized to further design and optimize the micro-groove structure and its distribution so that a dual directional backlight with proper directionalities and high uniformity can be obtained.

Chapter 3

Fabrication Technologies and Instruments

3.1 Introduction

The fabrication technologies available to fabricate the designed dual directional backlight components, such as diamond turning and plastic injection molding, will be briefly described in this chapter. As for the cost concern and time efficiency, however, the diamond turning is the most suitable one among the others.

After the fabrication, the characteristics and performance of the fabricated components and the designed dual directional backlight system, such as similarity to the geometric design, angular distribution and uniformity of the emitted light, were measured by an optical microscope (OM) and a Conoscopic system respectively. The features of the instruments mentioned above will also be illustrated later.

3.2 Fabrication Technologies

Nowadays there are various technologies to fabricate the structures of micro or nano scale [26]. They are generally called precision micromachining technology, whose classification is shown in Fig. 3.1. Most of them have many drawbacks, such as long turnover time, requirement of expensive equipments, limited materials types and profiles. The micro-mechanical machining is the one of less drawbacks and thus preferred as the fabrication tool here. In the following, the diamond turning technology, one of the micro-mechanical machining technologies, was chosen and described briefly. However, if mass production is desirable, replication is necessary for the cost concern. Therefore, the injection molding, which is popular in light-guide

fabrication, is also introduced right after the diamond turning.

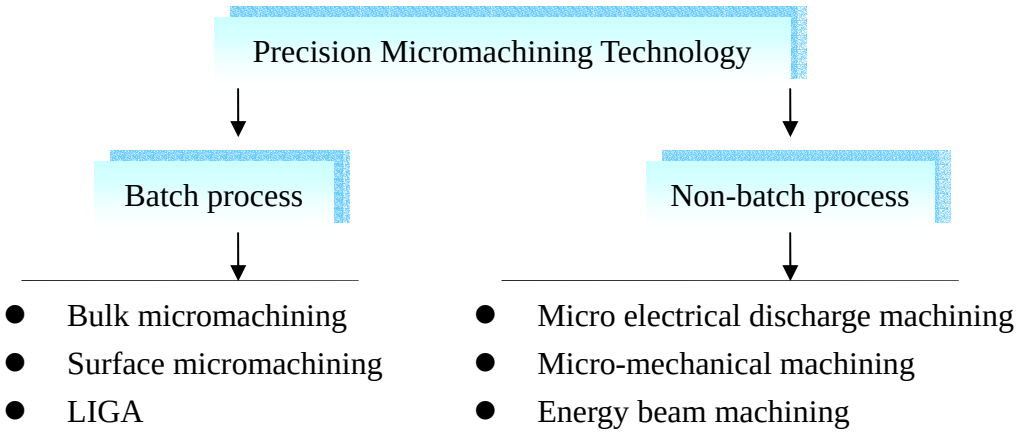

Fig. 3.1 Classification of Precision Micromachining Technology

3.2.1 Diamond Turning

Diamond turning [27], a kind of micro-mechanical machining, utilizes the copy principle to generate the desired structure. That means the track and shape of the diamond knife are completely transferred to the machined surface, as illustrated in Fig. 3.2. The profile accuracy and surface roughness are strongly determined by the qualities of the machinery, diamond knife, workpiece material and the environment. Under the best condition, the precision in profile and surface roughness may achieve 1um and 0.1 um (Rmax) respectively [28]. The suitable dimension of the micro structures ranges from a few to hundreds of micrometers.

The diamond turning provides a kind of fabrication process of low cost and high speed for small amount demand. Thus, it is appropriate to use the diamond turning to fabricate samples to verify the design goal.

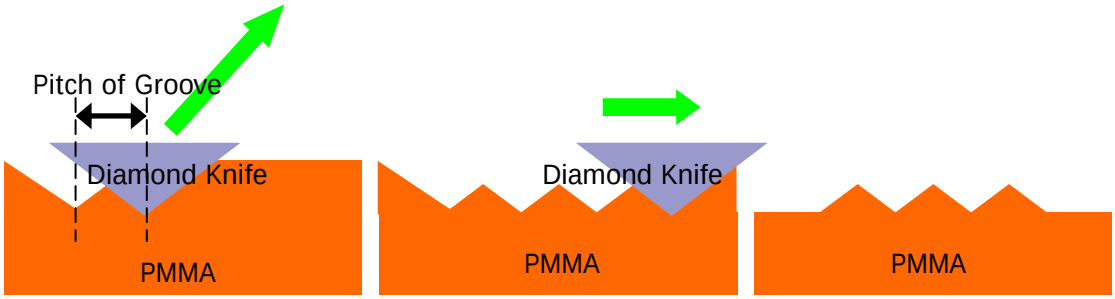

Step1:
Diamond knife was moved vertically to fabricate the groove.

Step2:
Diamond knife was moved horizontally to fabricate another groove.

Step3:
Edge parts of PMMA was removed by flattening

Fig. 3.2 Fabrication process of diamond turning

3.2.2 Plastic Injection Molding

The plastic injection molding has been applied in many fields, i.e. articles for daily use, containers, light-guides, optical lens, electronic products, etc. According to the mechanical actions of the mold, the injection molding process can be divided into five steps, including mold locking, injection, pressure preserved, cooling and ejection, as illustrated in Fig. 3.3[26]. After the plasticizing, i.e. the conversion of the polymer material from its normal hard granular form at room temperatures, to the liquid consistency necessary for injection at its correct melt temperature, this melt is introduced into a mold to completely fill a cavity or cavities. The action of removing heat from the melt to convert it from a liquid consistency back to its original rigid state is followed. As the material cools, it also shrinks. After the removal of the cooled, molded part from the mold cavity and from any cores or inserts, the after-treatment, such as baking and annealing, is often required to improve the stability of the finished products. In this way, the mass production of products is accomplished quickly and cost-effectively.

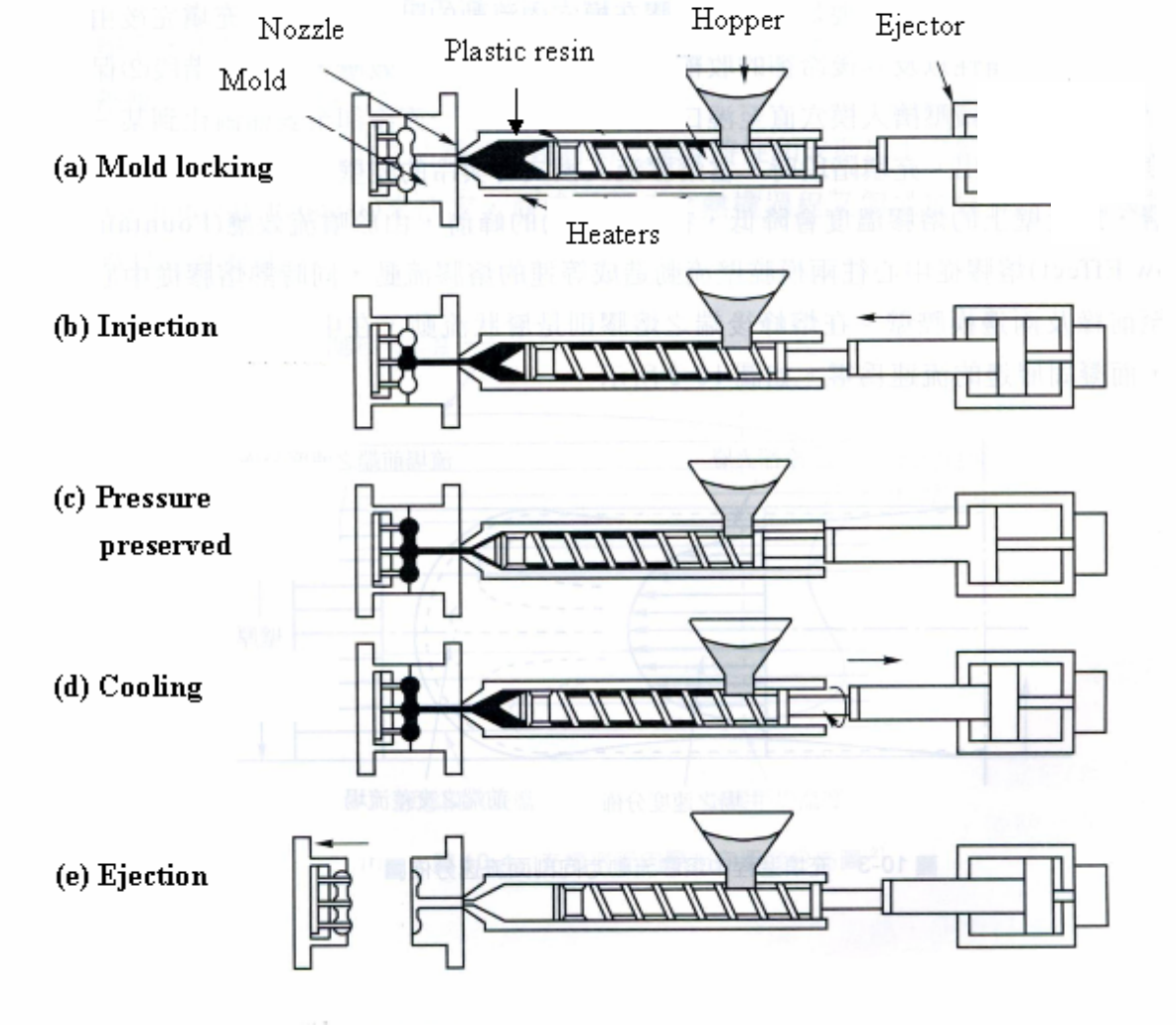

Fig. 3.3 Injection molding process: (a) mold locking, (b) injection, (c) pressure preserved, (d) cooling, and (e) ejection

3.3 Measurement Instruments

After the fabrication, we must make sure if the fabricated components meet the design goal. First, the geometric similarity to the designed structure is checked by the optical microscope (OM). Then, the optical performances of the fabricated components and designed dual directional backlight are measured by the conoscopic system which detailed descriptions are shown below.

Conoscope is a measurement system which utilizes Fourier transform lens to transfer the light beams emitted (or reflected) from the test area of different angles to the CCD array, as shown in Fig. 3.4. Every light beam emitted from the test area with a θ incident angle will be focused on the focal plane at the same azimuth and at a position x=F(θ). Therefore, the angular characteristics of the sample are thus measured simply and quickly, without any mechanical movement. Particularly, which kind of light source, i.e. collimated or diffuse illumination, is provided depending on the needs.

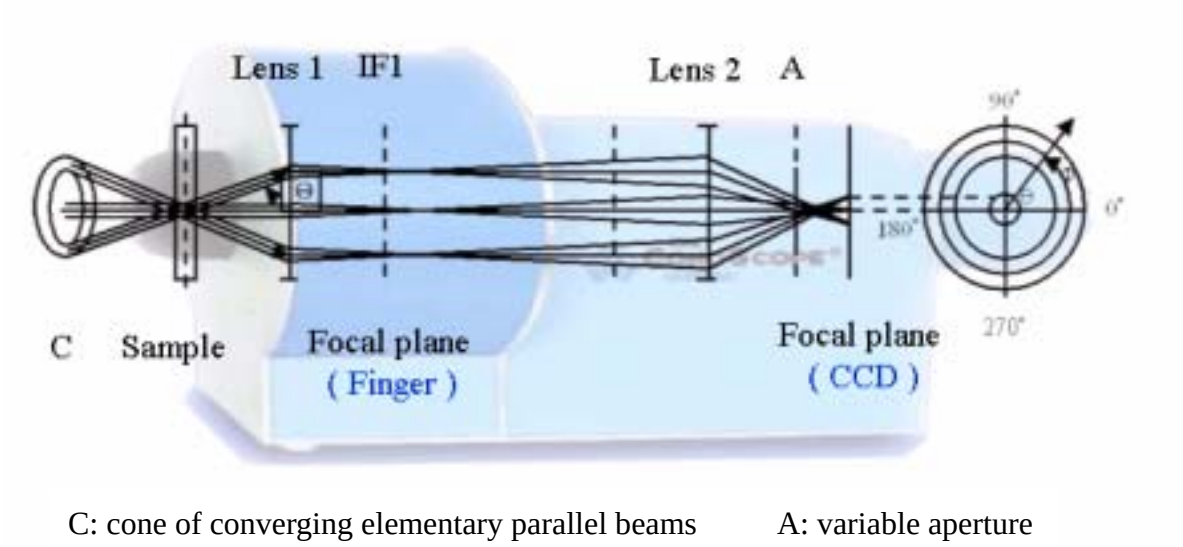

C: cone of converging elementary parallel beams A: variable aperture

Fig. 3.4 Schematics of Conoscope

Besides, by equipped with a fast photometer system and a high-sensitivity spectrometer, its functions are extended to comprise not only the simultaneous measurement of luminance and chromaticity versus viewing direction, evaluation of the data yields, i.e. luminance contras ratio, grey-scale inversion and reduction, color shift and many more characteristics, but also the spectra and temporal luminance variances.

Chapter 4

Simulated Results and Discussions

4.1 Introduction

Based on the principle described in chapter 2, we established a simulation model to characterize the features of the dual directional backlight system. First, the incident angle of the micro-groove structure was analyzed to produce proper directionalities. Besides, the groove structure, including groove pitch and groove depth, was varied in several regions or continuously to yield high uniformity. After that, the dual directional backlight system was designed and optimized. Further, a dual directional backlight for free of moiré` pattern was designed and optimized.

4.2 Simulation Software

The optical simulator Advanced Systems Analysis Program (ASAP™), developed by Breault Research Organization (BRO) was used to optimize the dual directional backlight system and simulate its angular distribution and light distribution on top surface of the backlight.

4.3 Simulation Model of Dual Directional Backlight System

In order to consider the whole effect on the dual directional backlight system, all the design and optimization processes were carried out under the complete system framework, as shown in Fig. 4.1. The simulation model consists of the main body of the dual directional backlight, i.e. two light sources, two directional light-guides and an absorber, and a fixed detector disposed right on the backlight. The light source

property in the simulation, as shown in Fig. 4.2, was set as a lambertian surface light source because a light bar of 4 light emitting diodes (LEDs) was used as a light source in application. The refractive index of the light-guides was set as 1.49 which is the same as that of PMMA. In addition, the top detector was set to detect the angular and spatial distributions of the emitted light, which were served as the bases of the optimizations.

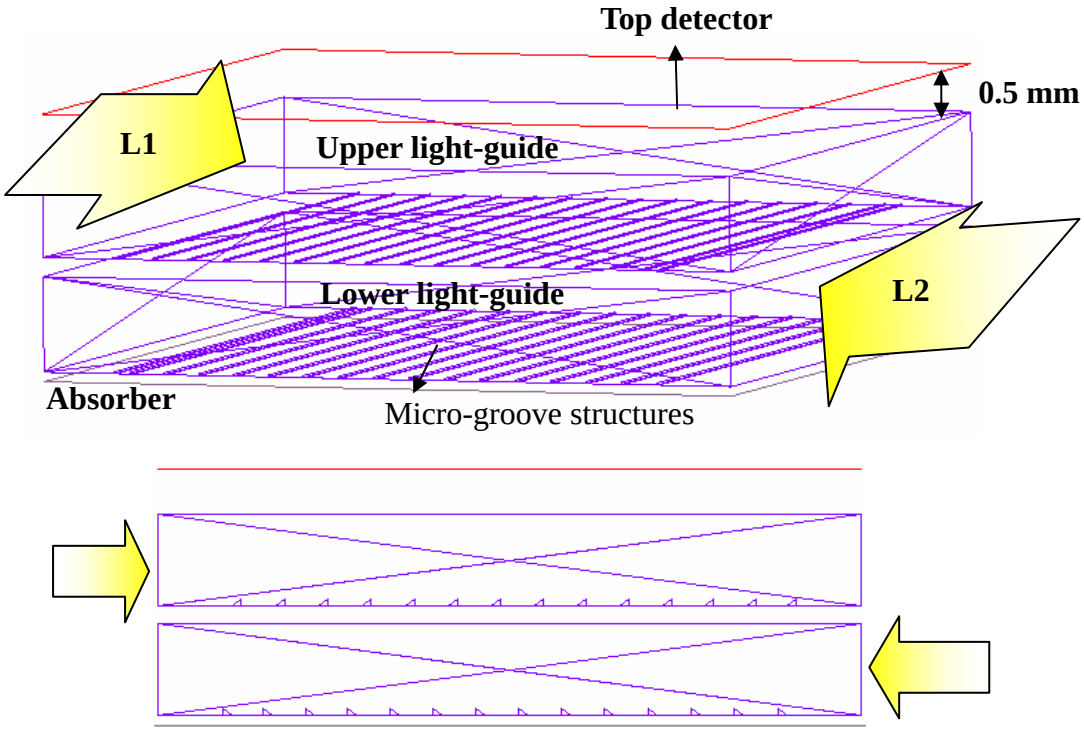

Fig. 4.1 Simulation model of the dual directional backlight system (not in the scale)

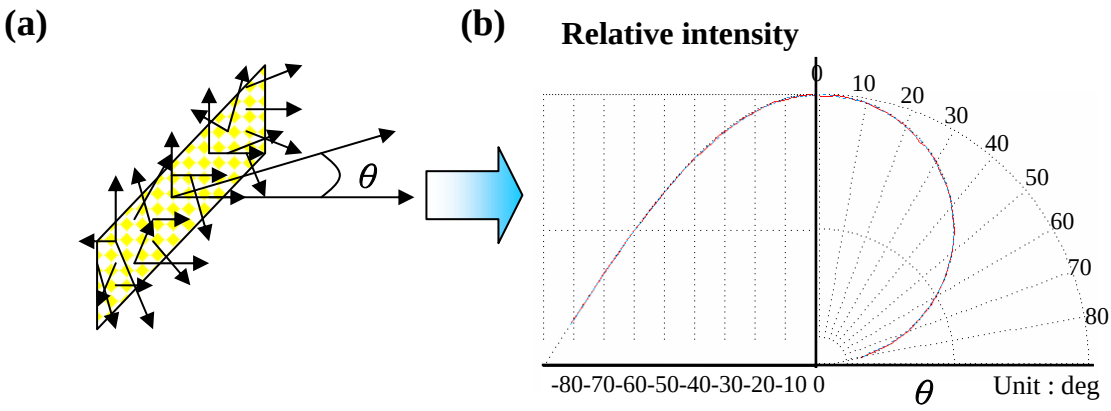

Fig. 4.2 Light source property in simulation: lambertian surface light source;
(a) simulated light source and (b) angular distribution of the simulated light source

In this thesis, a dual directional backlight system designed for 1.8” 3D mobile display was chosen, whose specifications were shown in Fig. 4.3. The light-guide size is 32 (W) × 38 (L) × 1 (H) mm^3 and the inner patterned area should be larger than display region, i.e.28 (W) × 35 (L) mm^2. Here, the light-guide thickness was determined by the available light bar size, i.e. about 1 (W) × 60 (L) mm^2. Ideally, however, the thinner the light-guide is, the higher the light efficiency is.

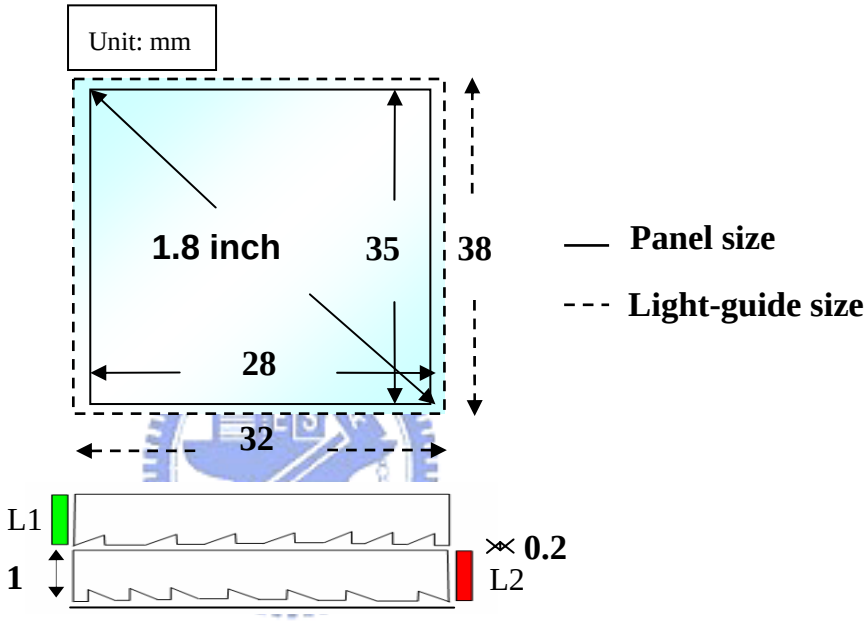

Fig. 4.3 Specifications of dual directional backlight system (1.8”)

4.4 Optimization of Dual Directional Backlight System

After established the simulation model, the next step is to optimize the parameters of the directional light-guide to obtain the desired optical performances. The parameters of the directional light-guide include the inclined angle of micro-groove structure, groove width and groove gap, as shown in Fig. 4.4. The inclined angle of the micro-groove structure, or called groove angle for short, affects the angular distribution of the emitted light and the groove pitch determines the light uniformity

which had been discussed briefly in chap 2. Before starting the optimizations, however, the proper optical performances are defined more clearly as in the following.

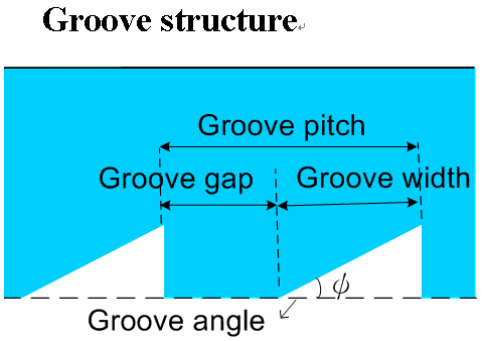

parameters		effected factor
Groove angle		angular distribution
Groove pitch	width	uniformity
	gap	

Fig. 4.4 Parameters of the directional light-guide and the effected factors

4.4.1 Optical Requirements of Dual Directional Backlight System

The important optical performances of the dual directional backlight are the angular distribution and the light uniformity which are discussed in detail below.

Angular distribution

In order to present images correctly, the angular distribution of the dual directional backlight must be well controlled into each viewing direction, which depends on the viewer` s position. In the time-multiplexed 3D mobile display, the viewer` s position can be predicted easily, roughly 10 to 40 cm normal from the display panel, and the corresponding angular distribution of backlight, suitable for viewing, can be calculated by geometry as shown in Fig.4.5. Here take the average distance between the pupils of the human eyes (65 mm) as an example. The corresponding viewing angle varies from $\pm 4.7^{\circ}$ to $\pm 18^{\circ}$. Therefore, most light must be guided to the two symmetrical viewing cones respectively and sequentially when the two light sources are fast switched.

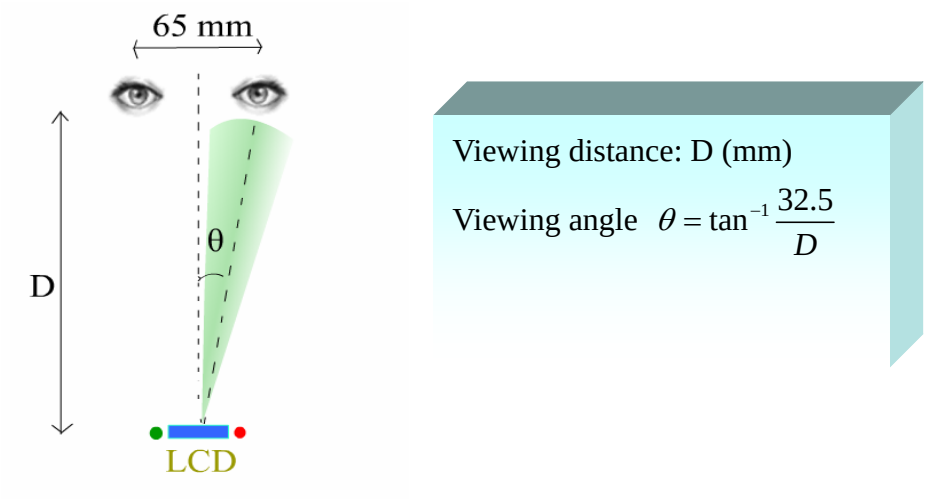

Fig. 4.5 Relationship between the viewing angle and the viewing distance

Moreover, the crosstalk should be as fewer as possible to yield good image qualities. Crosstalk results in the leakage of right and left eye images to the opposite eye, which not only degrades the picture quality of the stereoscopic images but is also thought to cause eyestrain and fatigue for the viewer. The crosstalk is defined as the ratio of brightness measured at one eye to the other. In general, crosstalk of less than 10% is the minimum criterion to produce stereoscopic image perception for our brain [28].

$$\text{Crosstalk} \equiv \frac{\text{luminance measured at one eye}}{\text{luminance measured at the other eye}} \qquad (4\text{-}1)$$

Uniformity

Uniformity influences not only the image quality of single eye but also the whole 3D effect. Here, the uniformity of brightness is defined as the ratio of the minimum to the maximum brightness. Uniformity of higher than 80% is generally required for commercial products.

$$\text{Uniformity} \equiv \frac{\text{min. luminance}}{\text{max. luminance}} \qquad (4\text{-}2)$$

4.4.2 Optimization of Groove Angle

In this section, the inclined angle of the micro-groove structure was optimized to obtain proper directionalities. As discussed above, the suitable angular distribution is located between ±4.7° to ±18°. Additionally, Table 2.1 shows the emitted angle of the horizontal incident ray is 15° when the groove angle is at 40°. Therefore, the angular distributions simulated under the various groove angles around 40°, i.e.38°, 39°, 40°, 41°and 42°, were examined. Figs. 4.6 (a) and (b) show these results for the light source 1 and 2 respectively. As seen in the figures, most light is distributed in a certain angular range with a peak when each light source is on. The peak of the angular distribution is closer to the normal direction as the groove angle gets larger. Besides, the peak width is larger as the groove angle gets smaller. The peak width at a smaller groove angle is wider because the incident angle range for TIR on micro-groove surfaces is larger. As a result, the angular distribution at groove angle 38° has the advantage of wider peak width compared with other angles. Another advantage of the angular distribution at groove angle 38° is the lower crosstalk which promises good directionalities. Most importantly, most of the peak values are located in the suitable angular distribution.

Although the angular distribution at groove angle 36°or 37° may have some better advantages, i.e. wider peak width and lower crosstalk, than that at groove angle 38°, the angular distribution at groove angle 38° is still the most suitable one due to its proper location. Therefore, the groove angle of 38°was used in the following optimization and the fabrication.

One thing needs to be pointed out is the simulated results mentioned above were carried out under a uniform distribution of micro-groove structures for convenience. The distribution of micro-groove structures dose not affect the directionalities but the

uniformity of backlight, which will be discussed next.

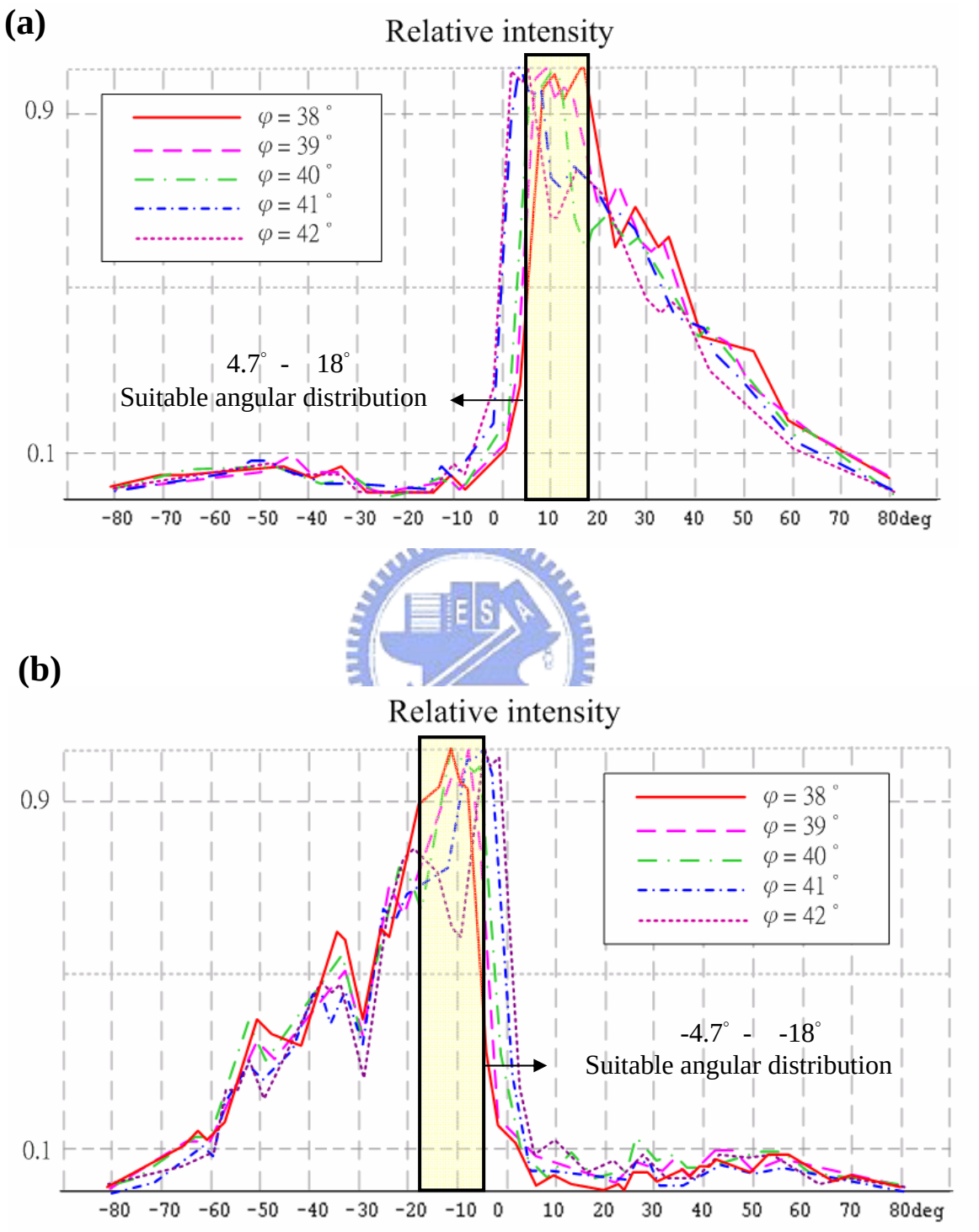

Fig. 4.6 Angular distributions at various groove angles when light source (a) 1 and (b) 2 is on, respectively

4.4.3 Optimization of Micro-groove Distribution

Because the light intensity decreases as the distance from light source increases, the micro-groove distribution must vary with the distance from the light source to enhance the uniformity. The basic principle is that the groove pitch closer to the light source should be larger than the farther one. In order to simplify the light-guide structure, the groove width can be fixed in whole patterned area, and the groove pitch is adjusted by varying groove gap. The optimization flow for micro-groove distribution is summarized in the following.

First, the patterned area was equally divided into a few regions. Secondly, choose the fixed groove width and vary the groove gap in each region to yield high uniformity. If the uniformity can not be improved by just varying each groove gap, changing the relative size of each region or using more regions is of help. Such steps were repeated several times until high uniformity was achieved. Thus, the distribution trend for high uniformity was found. Fig. 4.7 illustrates this optimization flow briefly.

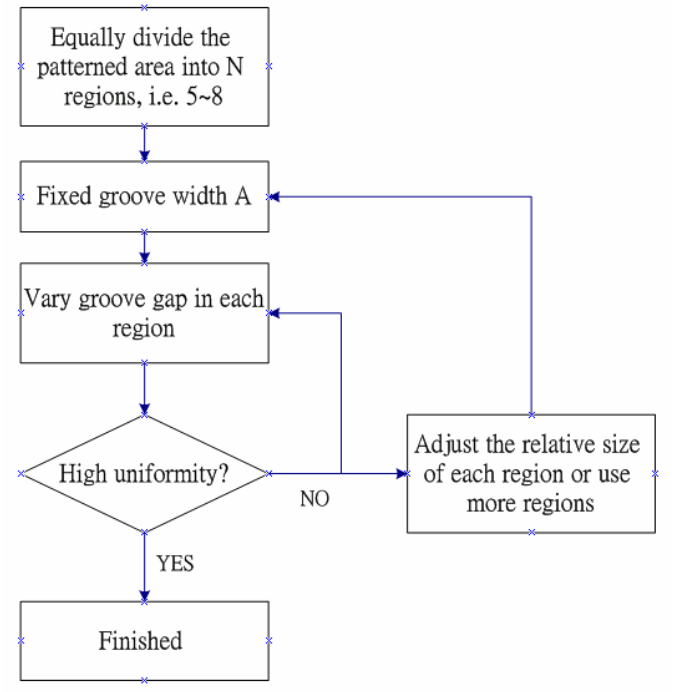

Fig. 4.7 Optimization flow of micro-groove distribution

In these processes, different groove width results in different light profile to meet specific needs. Because a smooth distribution with a smaller groove pith range can be obtained easily by using a smaller groove width, the groove width was chosen as 25 μm here to prevent visible groove pitches.

Follow the optimization flow described above and the corresponding distribution trend for uniformity of higher than 82 % was then found. In this optimized distribution, the groove gap was varied from 25 to 355 μm discretely and the distribution trend can be fitted by a quadratic function, as shown in Figs. 4.8 (a) and (b) respectively. The fitted quadratic function, written below Fig. 4.8 (b), can be further utilized to prevent discrete boundaries between each region. Figs. 4.9 (a) and (b) show the simulated spatial and angular distributions of the emitted light under this optimized distribution, where different color denotes different light intensity. As

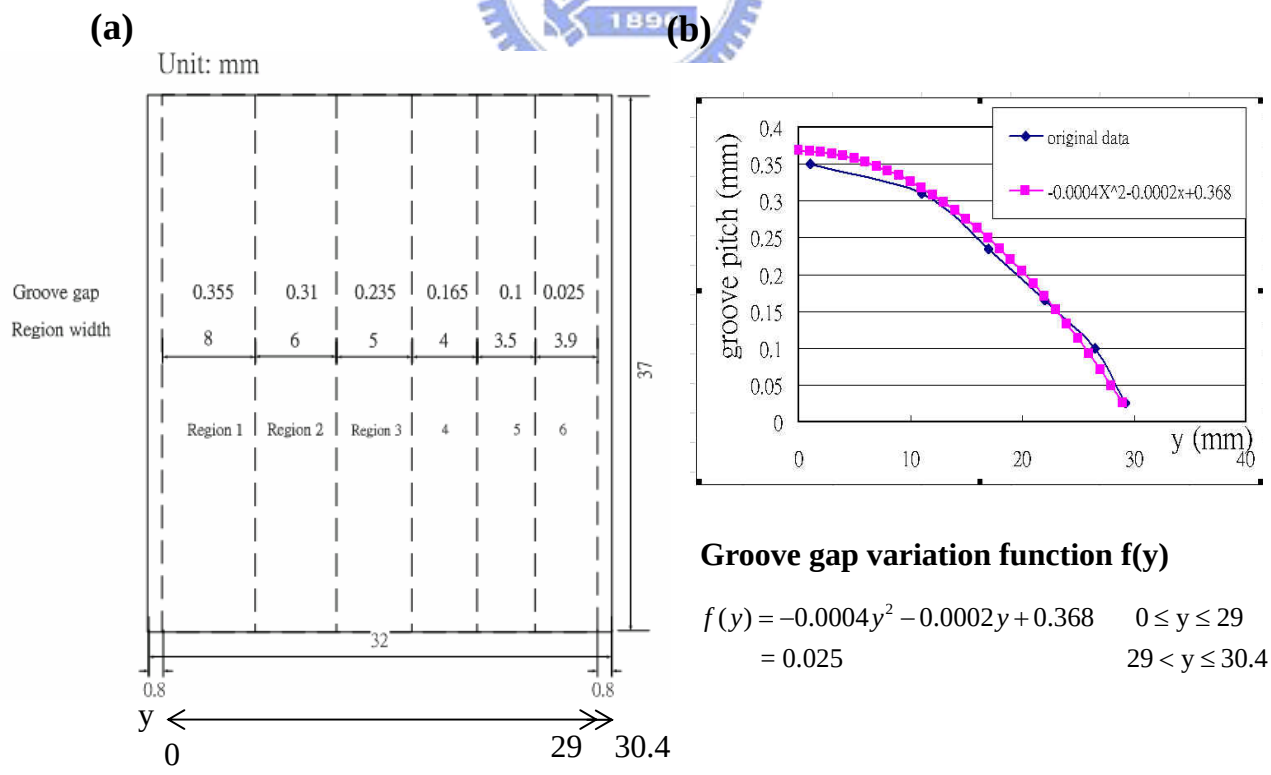

Fig. 4.8 (a) Optimized micro-groove distribution and (b) the corresponding distribution trend

shown in the color bar, red and blue denote the maximum and minimum intensity respectively. In addition, two orthogonal cross-section views were also provided besides the color map. According to the definition described in section 4.4.1, uniformity of higher than 82 % was achieved in both light sources while considering the display region only. Crosstalk of less than 10 % was located between ±6˚ and ±30˚, which was close to the desired angular distribution, ±4.7˚ to ±18˚.

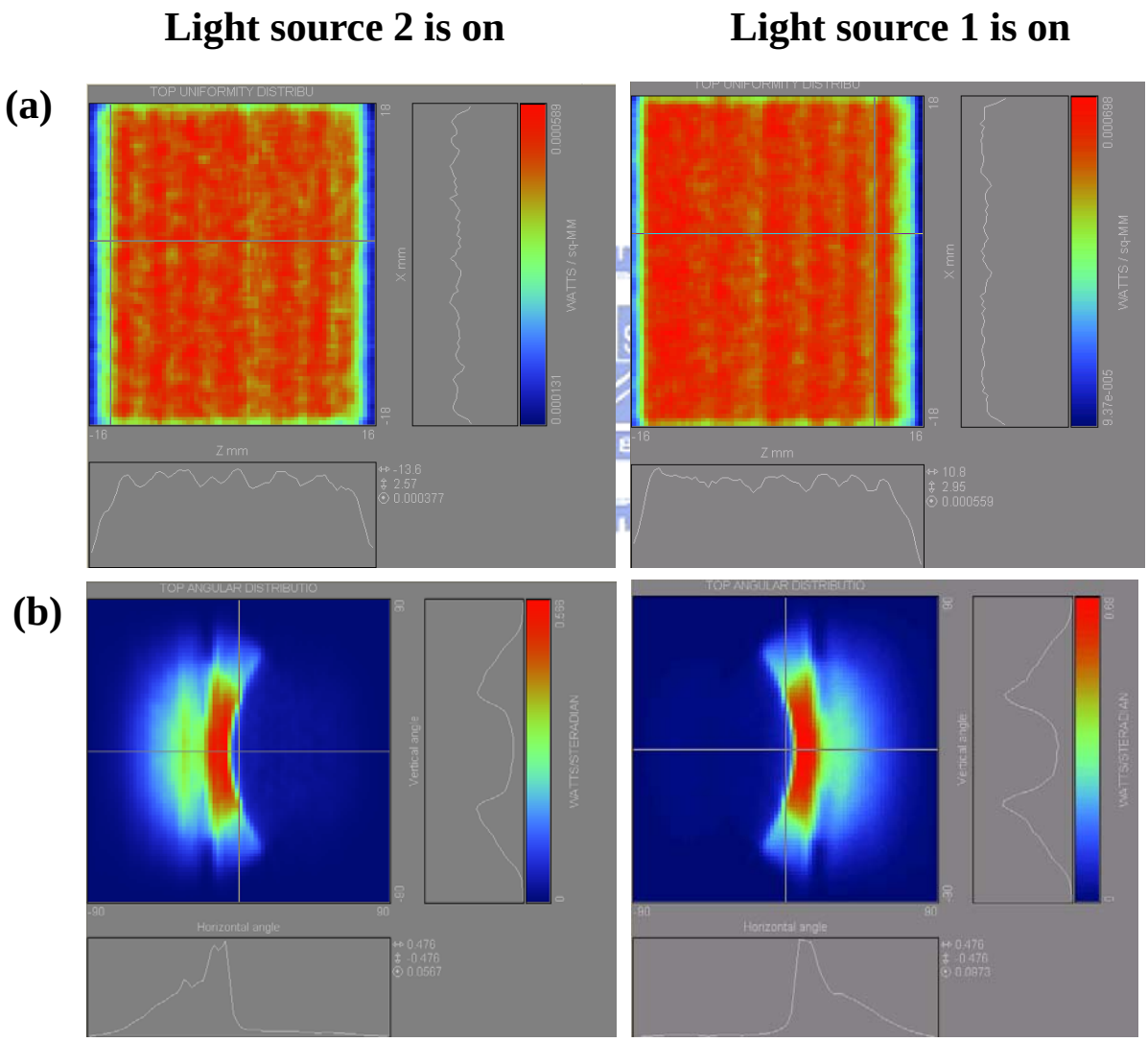

Fig. 4.9 Simulated (a) spatial and (b) angular distributions under discrete micro-groove distribution

In order to prevent the discrete boundaries between each region and achieve higher uniformity, the continuous micro-groove distribution characterized by a quadratic function, as shown in Fig. 4.8 (b), was further simulated and examined. Figs. 4.10 (a) and (b) show the simulated spatial and angular distributions of the emitted light, respectively. As seen in the figures, uniformity was indeed improved by the continuous distribution and the angular distribution was almost the same as that in the discrete distribution. Uniformity of higher than 84 % and crosstalk of less than 10 % between ±6° and ±30° were achieved. Figs. 4.11 (a) and (b) show the simulated discrete and continuous distributions of the micro-groove structures, respectively, where no discrete boundaries exist in the continuous distribution. Therefore, the

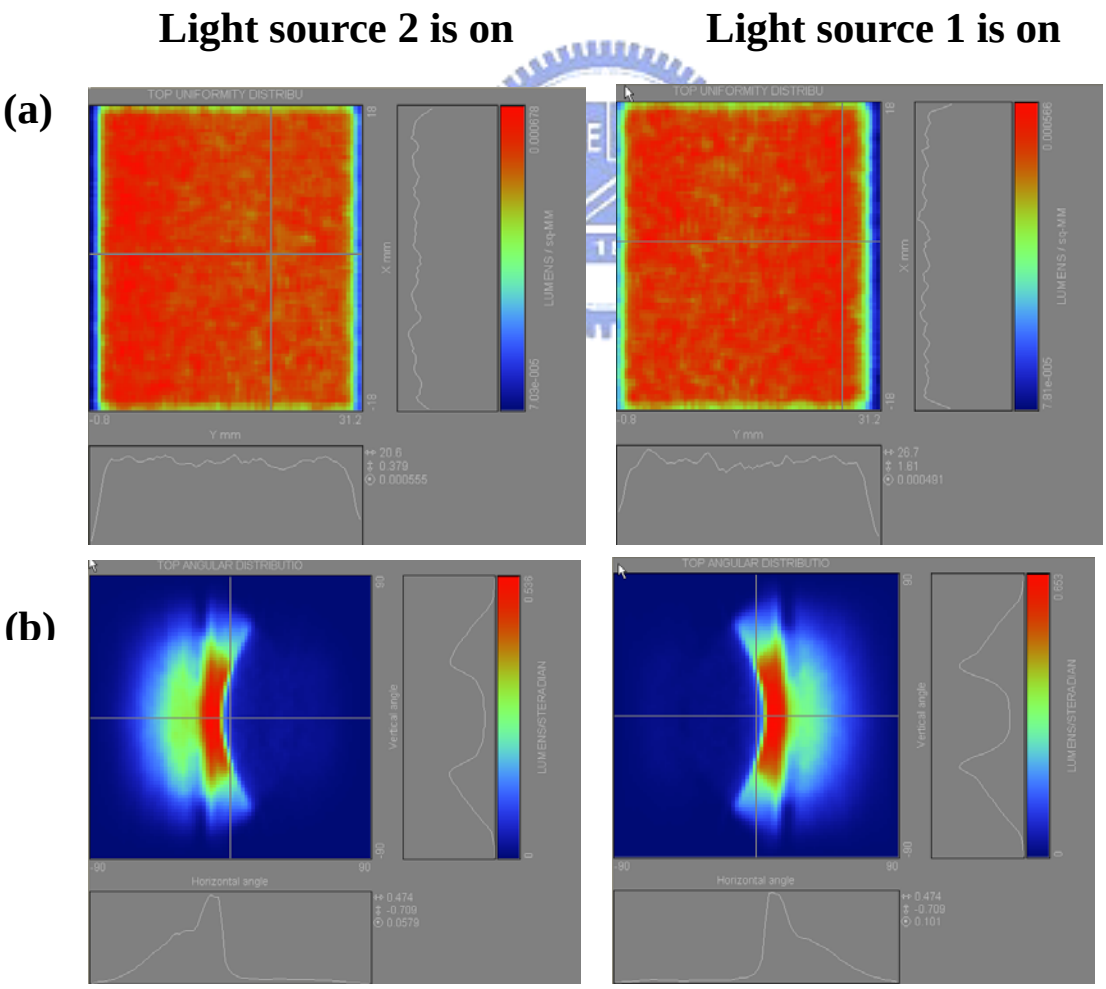

Fig. 4.10 Simulated (a) spatial and (b) angular distributions under continuous micro-groove distribution

(a) Discrete distribution (b) Continuous distribution

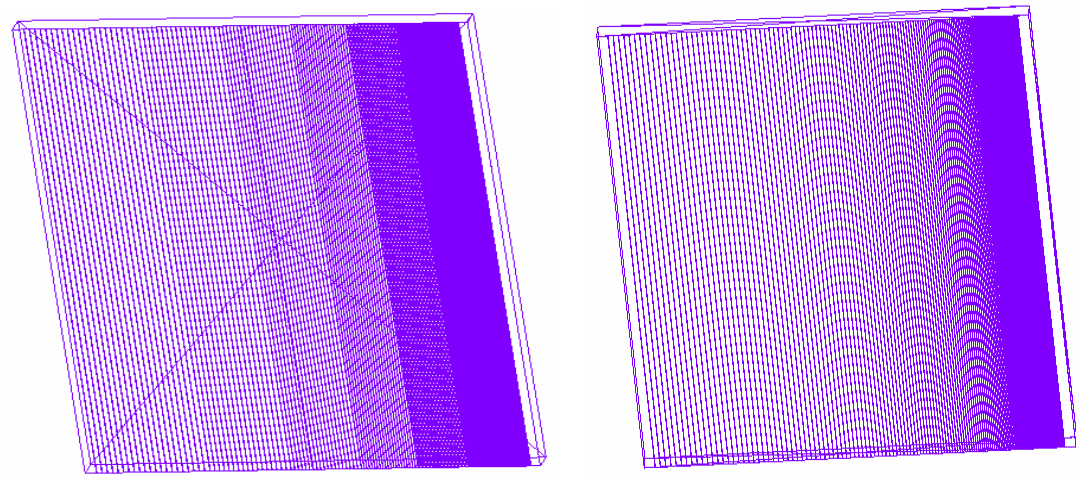

Fig. 4.11 Simulated (a) discrete and (b) continuous distributions of the micro-groove structures on the directional light-guide

continuous distribution was adopted and put into fabrication.

4.5 Design for Free of Moire` Pattern

In this section, a dual directional backlight for free of moiré` pattern was designed and optimized. When the LC panel and the directional light-guides with continuous distribution are superposed, serious moiré` pattern appear in the regions where the pitch ratio of the two overlapped structures is close to 1 or 2. In ASAP, this situation can be simulated by adding a RGB array, similar to a color filter, right on the top surface of the backlight, as shown in Fig. 4.12. The pitch of the RGB array was set as that of the color filter, i.e. 220 μm. As seen in the figure, serious moiré` pattern appear in the region of groove pitches close to 220 $\mu$m. The moiré` pattern in the region of groove pitches close to 110 μm also exists, but is almost invisible due to the tiny pattern pitches. Therefore, a discrete micro-groove distribution, exclusive of the groove pitches close to 220 μm, must be adopted to suppress the moiré` pattern.

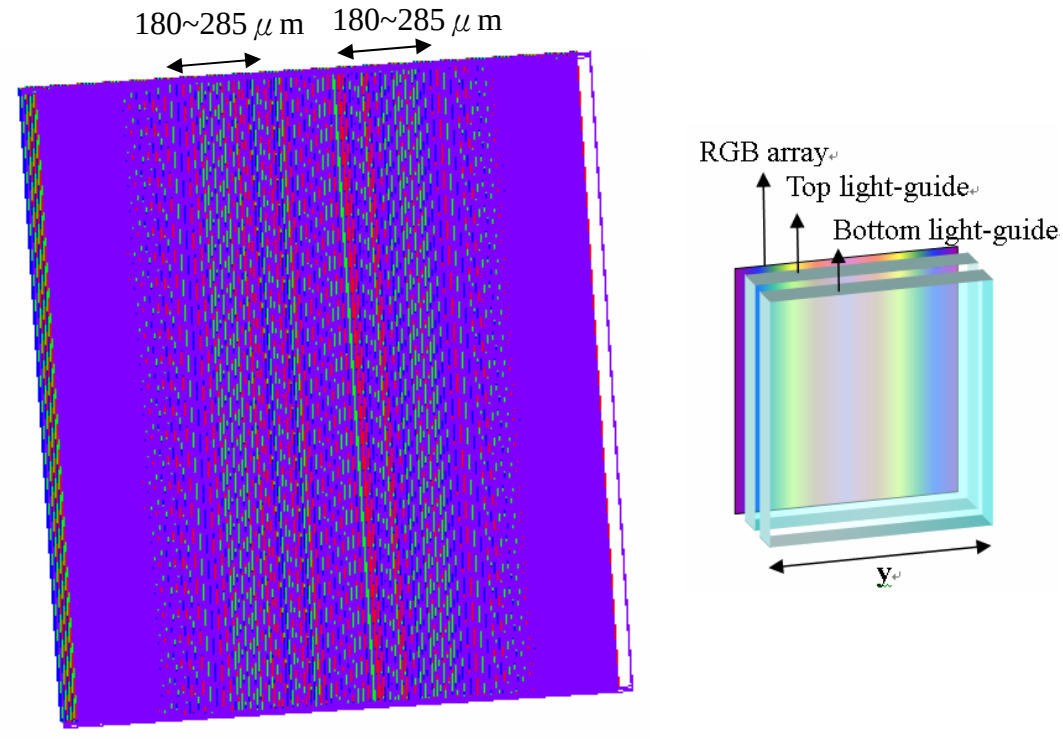

Fig. 4.12 Simulated directional light-guides with a RGB array on the top

Referred to the optimization processes and the optimized distribution trend mentioned above, the new design for free of moiré` pattern can be optimized as in the following. First, the patterned area was also divided into a few regions. Then the groove pitch in each region was varied to yield high performance, as done in the previous section. In this design, however, the groove width must be smaller and varied in some regions to achieve high uniformity. Finally, the discrete distribution was optimized, as shown in Table 4.1. The groove gap was varied from 20 to 290 μm while the groove width was varied around 20 μm. Fig. 4.13 shows the simulated directional light-guides with such micro-groove distribution and a RGB array on the top. Compared with Fig. 4.12, moiré` pattern was suppressed markedly in this new design. Besides, the optical performances are not compromised, as shown in Figs. 4.14 (a) and (b). Uniformity of higher than 83 % and crosstalk of less than 10 % between $\pm 6.5^{\circ}$ and $\pm 35^{\circ}$ were achieved.

Table 4.1 Optimized micro-groove distribution for free of moiré` pattern (unit: mm)

y	groove gap / width	y	groove gap / width	y	groove gap / width
0 - 4.5	0.29 / 0.019	17.5 - 19.5	0.16 / 0.019	25.5 - 26.5	0.07 / 0.02
4.5 - 8.5	0.283 / 0.019	19.5 - 21.5	0.15 / 0.019	26.5 - 27.5	0.055 / 0.02
8.5 - 11.5	0.273 / 0.02	21.5 - 23.5	0.125 / 0.02	27.5 - 28.5	0.042 / 0.02
11.5 - 14.5	0.269 / 0.023	23.5 - 24.5	0.105 / 0.02	28.5 - 29.5	0.032 / 0.02
14.5 - 17.5	0.265 / 0.024	24.5 - 25.5	0.085 / 0.02	29.5 – 30	0.02 / 0.02

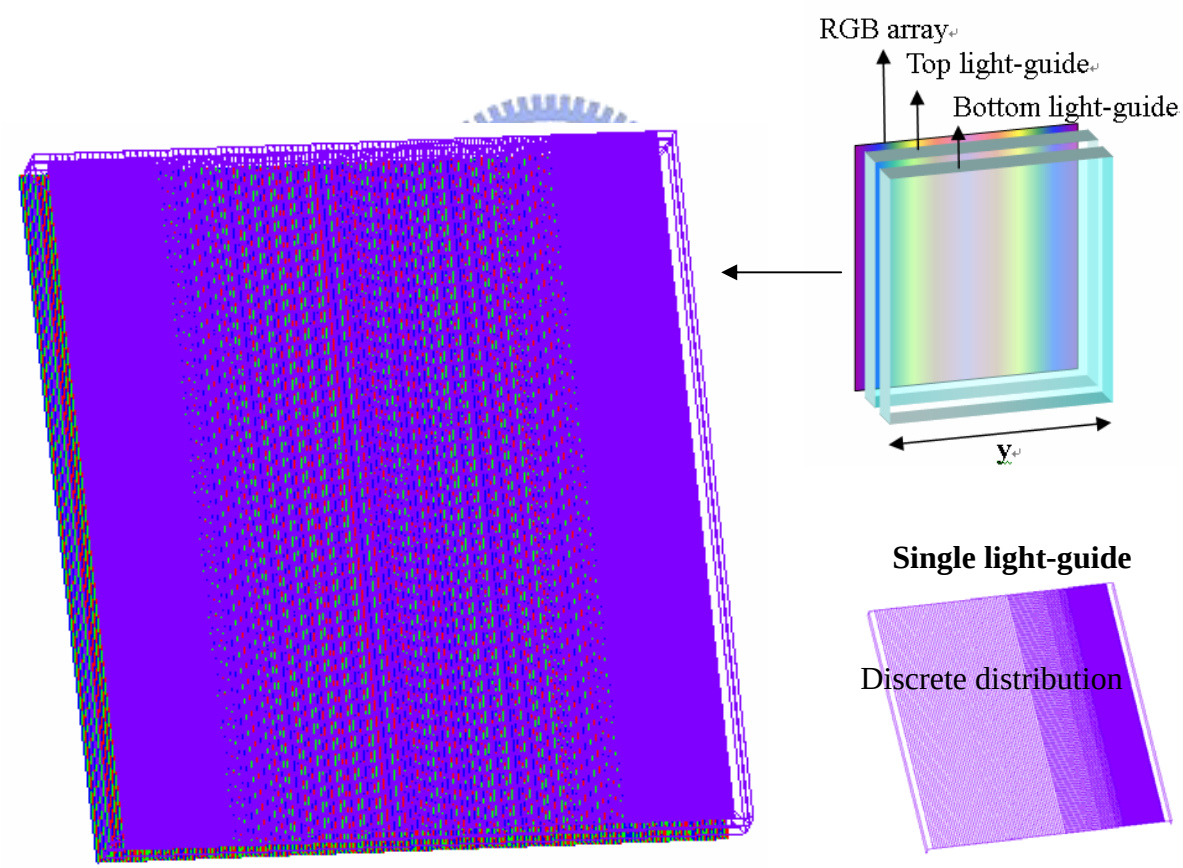

Fig. 4.13 Directional light-guide for free of moiré` pattern s with a RGB array on the top

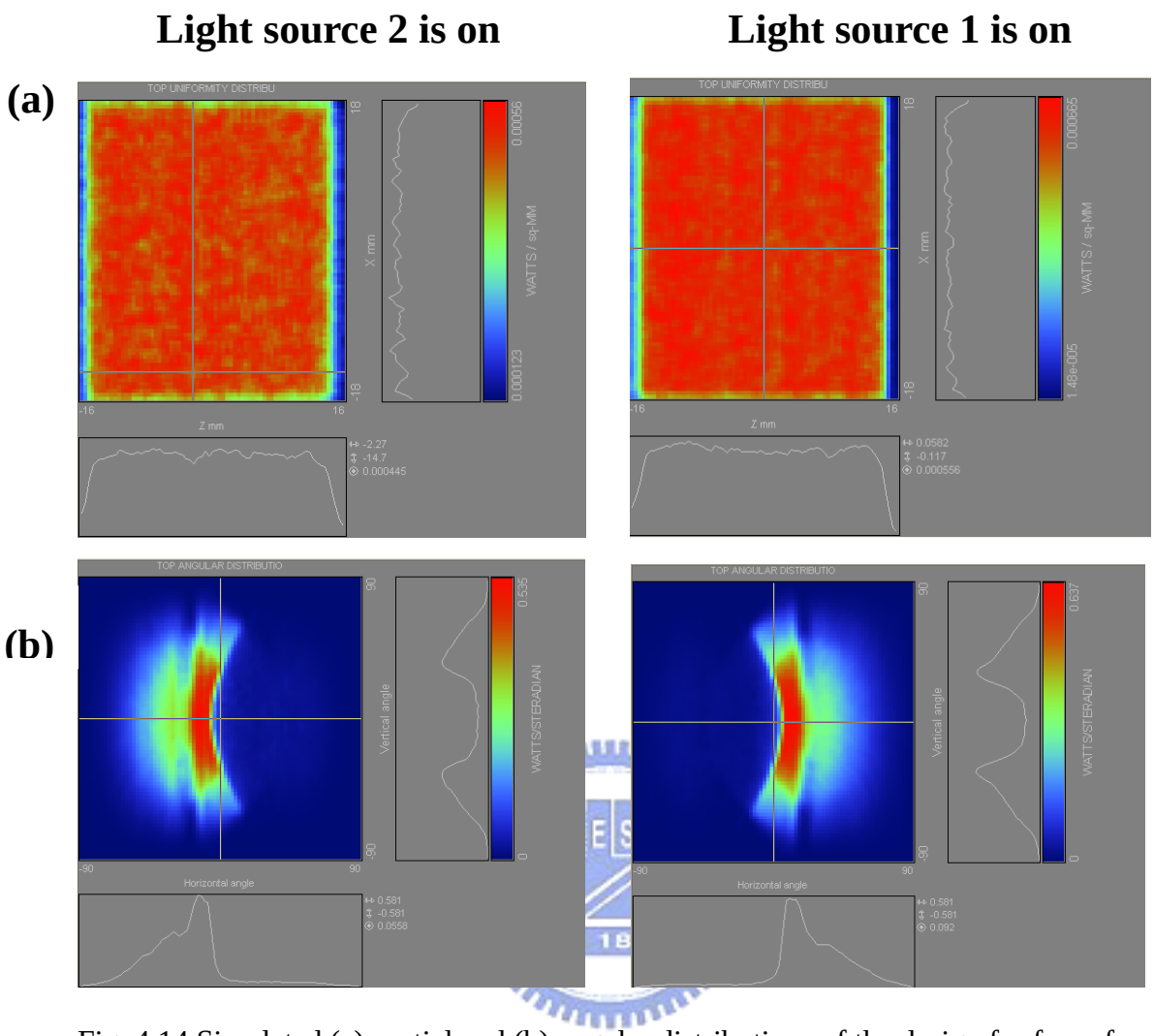

Fig. 4.14 Simulated (a) spatial and (b) angular distributions of the design for free pf moire` pattern

The discrete distribution trend of the dual directional backlight for free of moiré` pattern can be further fitted by three functions in different parts, as shown in Fig. 4.15. Again, in order to prevent the discrete boundaries between each region, the new partial continuous distribution characterized by these three functions was simulated and examined. In order to keep high uniformity, the groove width was varied, similar to that in previous one, and also shown in Fig. 4.15. Similarly, directional light-guides with partial continuous distribution and a RGB array on the top were simulated, as shown in Fig. 4.16, whose appearance is smoother than Fig. 4.13. Figs. 4.17 (a) and (b) show the simulated spatial and angular distributions of emitted light, respectively.

Uniformity of higher than 84 % and crosstalk of less than 10 % between ±6.5° and ±35° were achieved. Therefore, the partial continuous distribution was adopted as the design for free of moiré` pattern and put into fabrication due to the better performances.

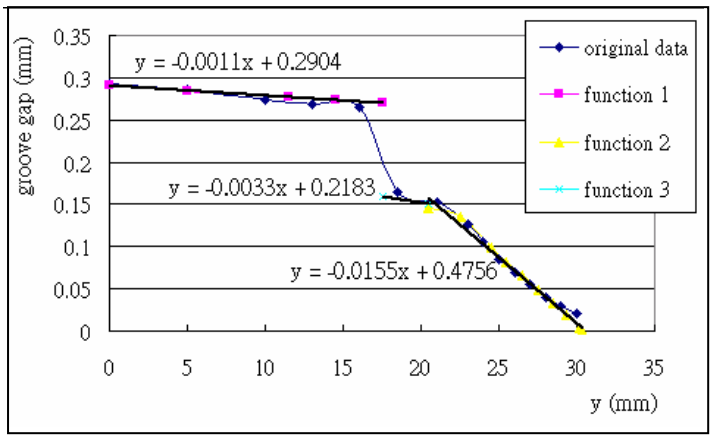

Groove gap variation function f(y)

$$f(y) = \begin{cases} -0.0011y + 0.2904 & 0 \le y \le 17.5 \quad \text{(fun 1)} \\ -0.0033y + 0.2183 & 17.5 \le y \le 20.5 \quad \text{(fun 2)} \\ -0.0155y + 0.4756 & 20.5 \le y \le 30.4 \quad \text{(fun 3)} \end{cases}$$

Unit : mm

y	0 - 7	7 - 12	12 - 15	15 - 17	17 - 20.5	20.5 – 22.5	22.5 – 27	27– 30.4
Groove width	0.019	0.021	0.024	0.027	0.018	0.021	0.022	0.024

Fig. 4.15 Fitted functions for the micro-groove distribution in the design for free of moiré` pattern

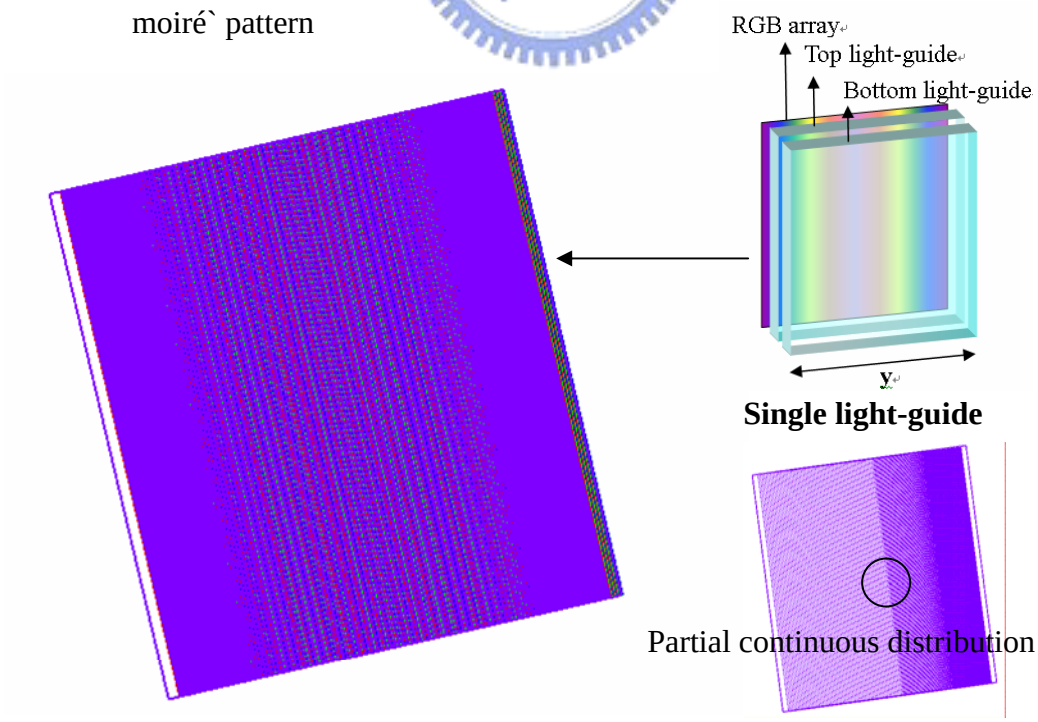

Fig. 4.16 Directional light-guides with partial continuous distribution and a RGB array on the top

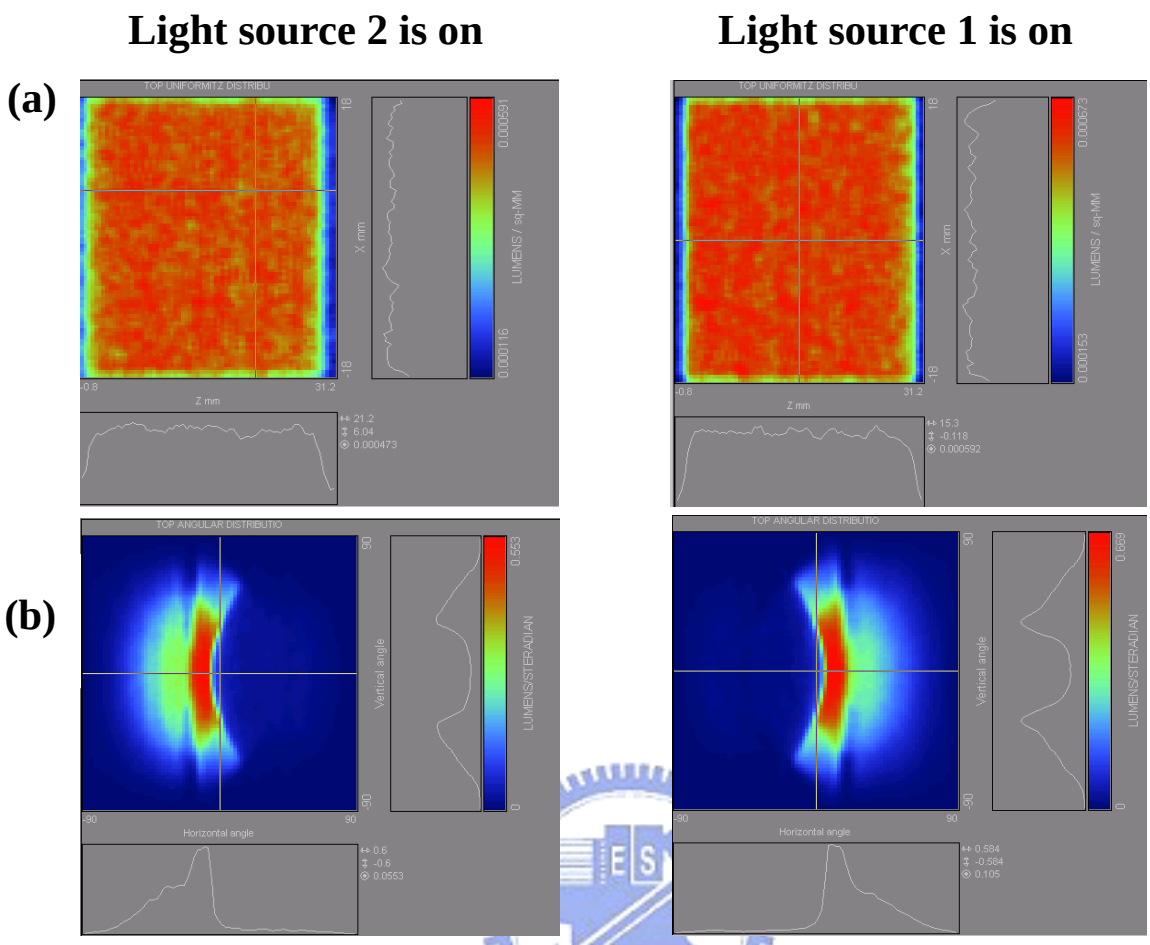

Fig. 4.17 Simulated (a) spatial and (b) angular distributions of the design for free of moiré` pattern

4.6 Summary

The micro-groove structure and distribution on the directional light-guide have been designed and optimized. It is recognized from the simulated results and analyses that the dual directional backlight using two directional light-guides can yield uniform light in the specific directions. In general, uniformity of higher than 84 % and crosstalk of less than 10 % between $\pm 6.5^\circ$ and $\pm 30^\circ$ were achieved. The corresponding viewing distance, suitable for 3D vision, varies from 4.6 to 28.5 cm. Moreover, a dual directional backlight for free of moiré` pattern was also obtained without compromise of the optical performances.

Chapter 5

Experimental Results and Discussions

5.1 Introduction

The characteristics of the fabricated directional light-guides were examined and discussed in this chapter. The optimized directional light-guides with continuous micro-groove distribution and those with partial continuous distribution were fabricated by diamond turning, whose specifications are the same as shown in chap 4. After that, an optical microscope (OM) was utilized to examine the fabricated structures. The important optical performances of the backlight module with the fabricated directional light-guides, such as angular distribution and luminance, were measured by Conoscope. Due to the directionalities and small size of backlight, the optical performances were measured at five points, which were randomly chosen from the five specified regions on backlight, as shown in Fig. 5.1. In addition, the suitable viewing distance for 3D vision was further calculated according to the definition mentioned in chap 4. Finally, the optical performances of the two fabricated designs are compared.

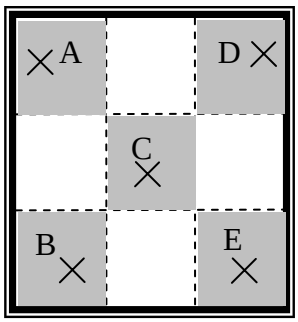

$$\text{Uniformity} = \frac{\min(A,B,C,D,E)}{\max(A,B,C,D,E)}$$

A,B,C,D,E: peak luminance measured at five specified regions

Fig. 5.1 Calculation of uniformity

5.2 Light Source Properties

A light bar of 4 white LEDs was used as one light source, whose angular distribution affects the angular distribution of backlight and was measured by Conoscope. Fig. 5.2 (a) shows the angular distribution of the light bar is almost circularly symmetric. Besides, most emitted light of the light bar centralizes within ± 30° due to the modification of the light-guide inside the light bar, as shown in Fig. 5.2 (b). Although the angular distribution of the light bar is different from that used in the simulation, i.e. lambertian type, such angular characteristic is better because it contributes more light to the TIR region, which increases the peak value of the angular distribution of backlight.

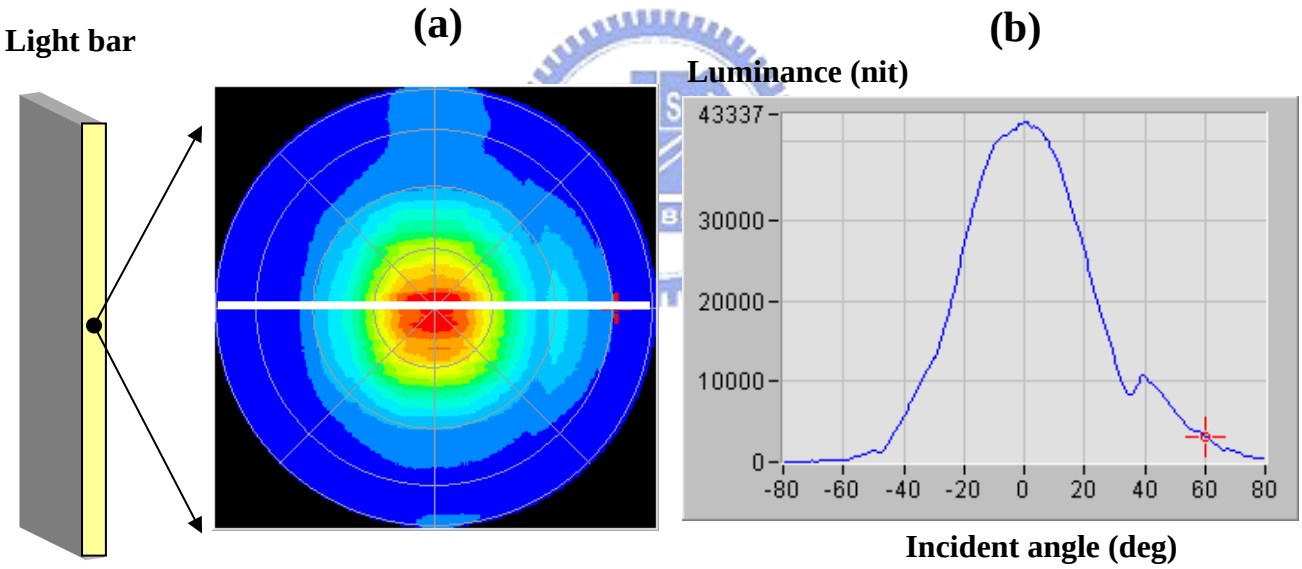

Fig. 5.2 (a) Measured angular distribution of the light bar and (b) its cross-section

5.3 Measured Results of the Dual directional Backlight with Continuous Micro-groove Distribution

5.3.1 Micro-groove profiles

After the fabrication, OM was utilized to verify the fabricated micro-groove structures on the light-guide first. Fig. 5.3 shows the measured micro-groove profiles where the coordinate

axis, y, is the same as that in the simulation. As seen in Fig. 5.3, the micro-groove profiles are rugged and vary from place to place. As a result, only three of them are presented here. The departures from the designed groove angle of 38° and groove width of 25 μm are approximately within ±6° and ±10 μm respectively and mostly resulted from the stress in the fabrication process. Full discussion about the influences of these departures on the angular distribution and uniformity of the dual directional backlight will be presented later.

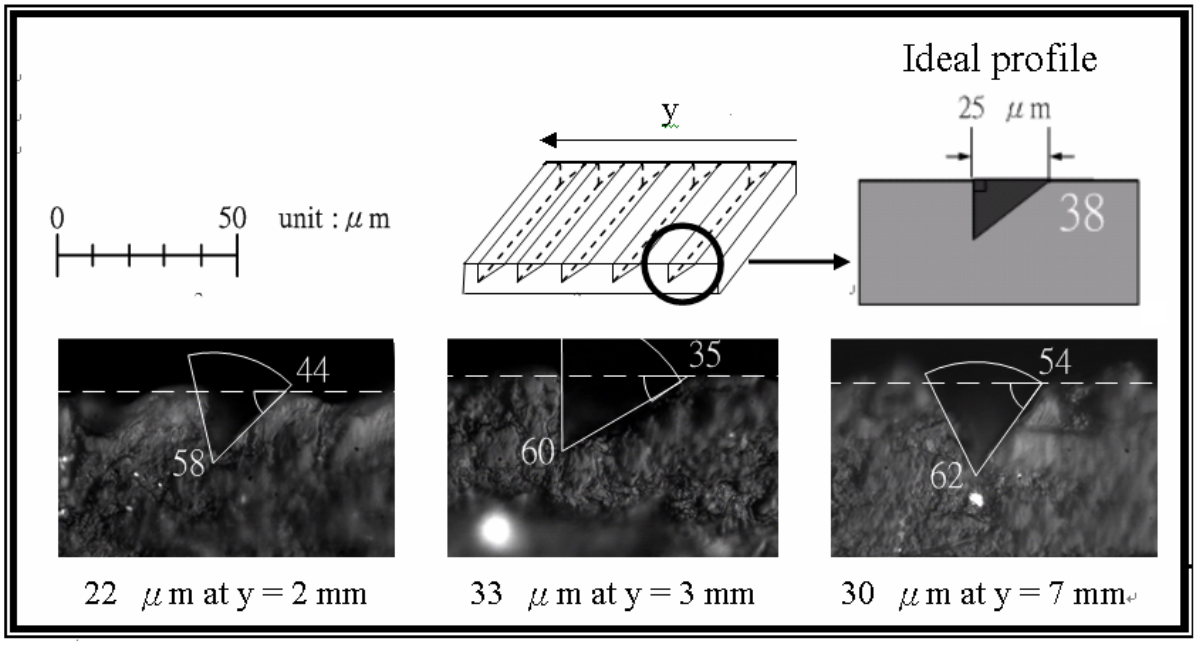

Fig. 5.3 Micro-groove profiles measured at different positions

5.3.2 Optical Performances

For the dual directional backlight, the optical performances at five different positions, as shown in Fig. 5.1, were measured and discussed. The experiment setup to measure the optical performances of the dual directional backlight was illustrated in Fig. 5.4. Here, a sheet of black paper was used as an absorber, and a diffuser sheet of low Haze, about 30%, was added on the top of the backlight system to soften the marked directionality of the micro-groove structures and the corresponding sensible micro-groove pattern image. The measured angular distributions of the dual

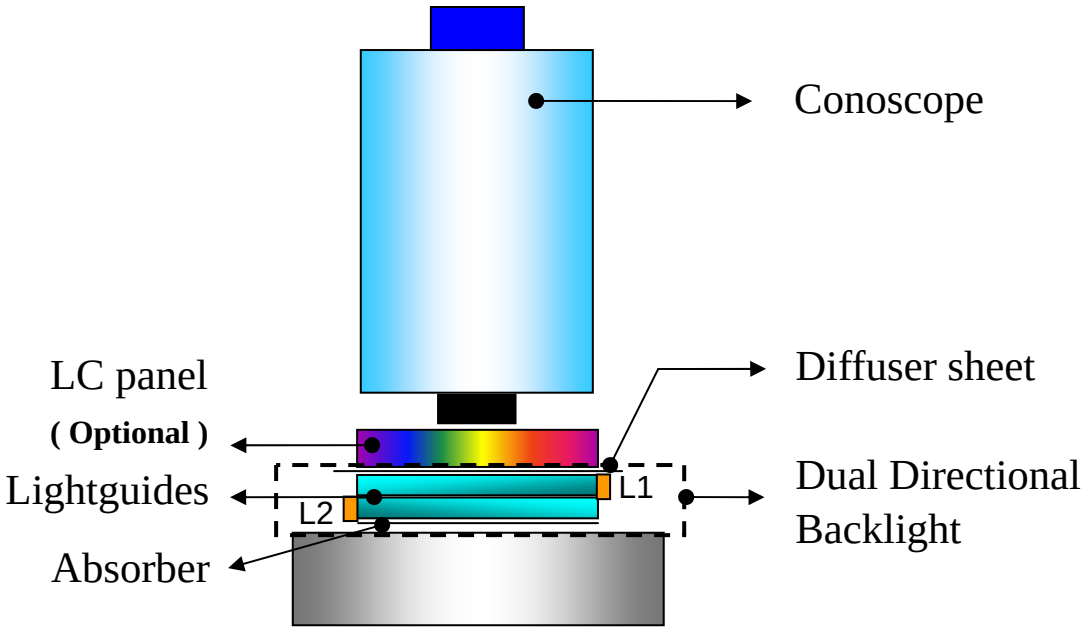

Fig. 5.4 Experimental setup for the optical performances of dual directional backlight

directional backlight for L1and L2 are shown in Fig. 5.5 and Fig. 5.6, respectively, where the regions with crosstalk of less than 10 % were also shown. After analyses, the angular distributions for L1 and L2 behave similarly in three aspects, as described in the following.

(1) **The amount of the light emitted at large angle decreases as the distance from the light source increases** because the emitted light of large angle is originated from the incident rays of large angle, which mostly penetrate and leave the light-guides in the forward part of the light-guides.

(2) **The appearance of the angular distribution only varies with the distance from the light source due to the asymmetry of the micro-groove pattern.**

(3) **Most light distributes in a certain viewing cone, i.e. 10° to 20° or -10° to -20°, thus, crosstalk is low.**

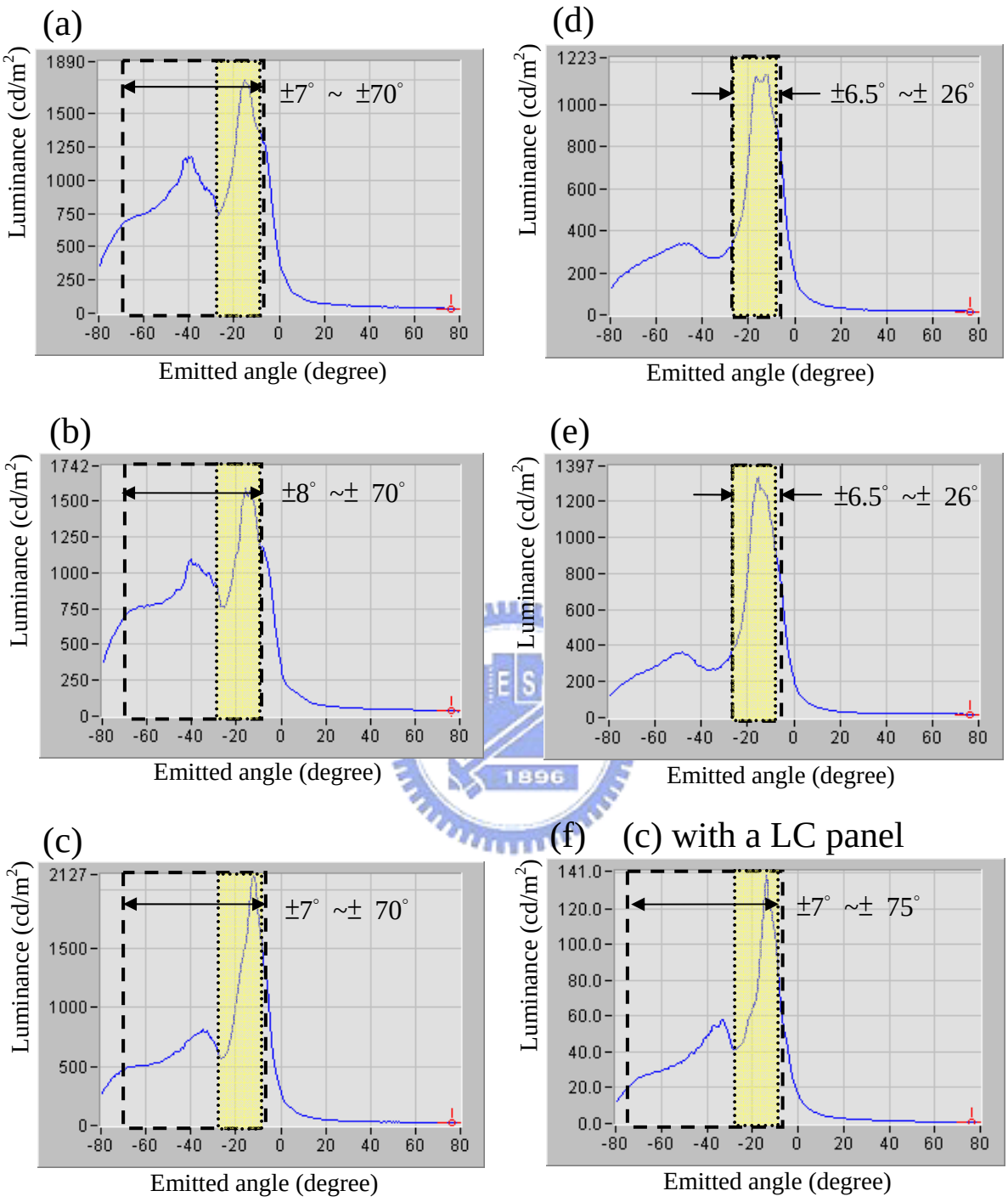

Fig. 5.5 Angular distributions of L1 measured at different positions on backlight: (a) above left, (b) below left, (c) center, (d) above right, (e) below right, and (f) (c) with a LC panel. Crosstalk of less than 10% is located in the region marked by dash line. Suitable angular distribution for 3D vision, ±8° to ±26°, is marked by dotted line.

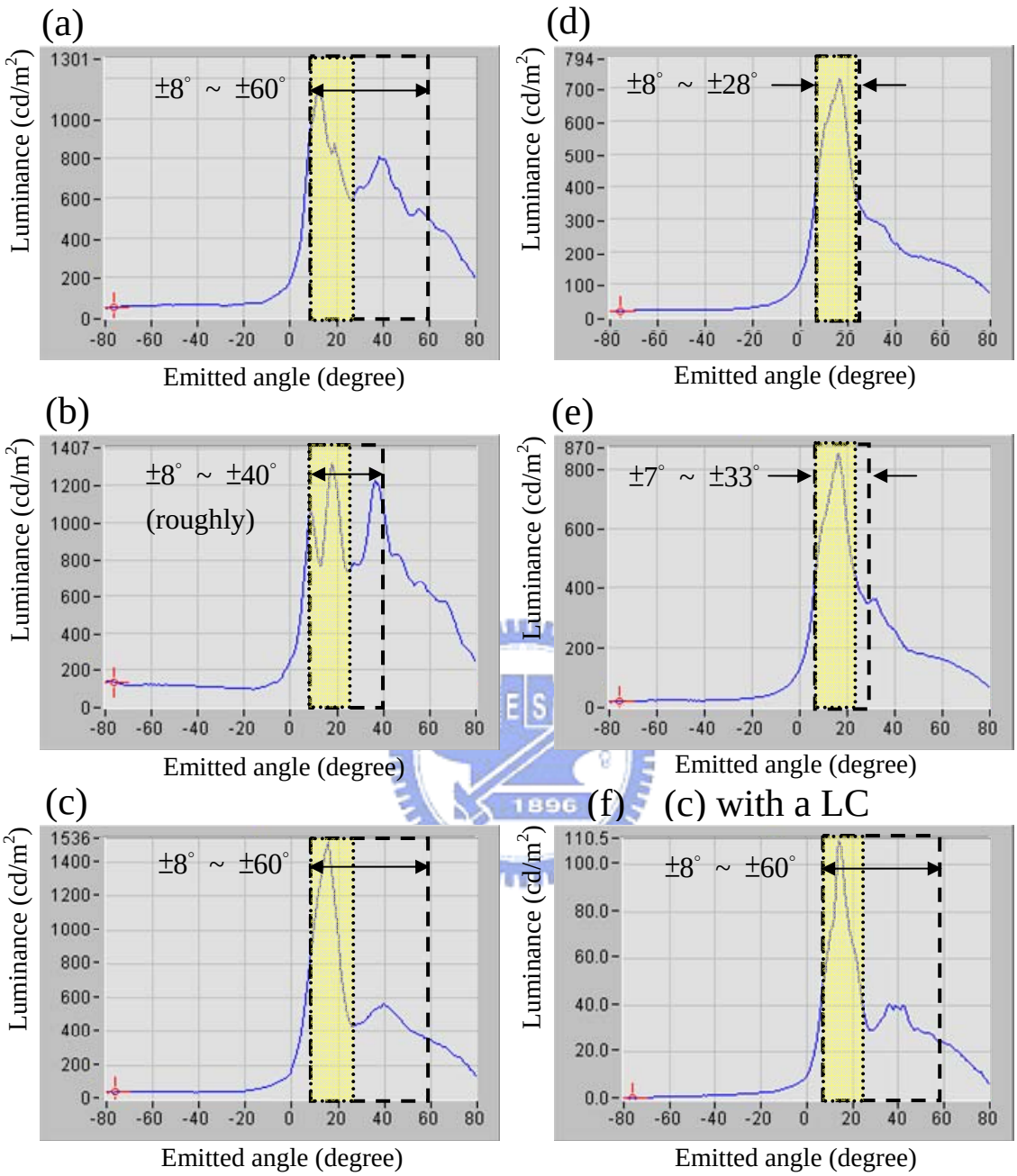

Fig. 5.6 Angular distributions of L2 measured at different positions on backlight: (a) above left, (b) below left, (c) center, (d) above right, (e) below right, and (f) (c) with a LC panel. Crosstalk of less than 10% is located in the region marked by dash line. Suitable angular distribution for 3D vision, ±8° to ±26°, is marked by dotted line.

The common features described above originate from the intrinsic characteristics of the designed directional light-guide. Another intrinsic feature is that more light leakage happens in the area close to the light source when L2 is turned on. The reason is the emitted light from the bottom light-guide may be totally reflected by the surfaces of β, an angle close to 90° on the top light-guide to the opposite direction, as shown in Fig. 5.7. This condition happens more easily in the region close to L2 due to that with more densely distribution of micro-groove structures on the top light-guide. However, the leakage amount close to the light source 2 is acceptable, as seen in Figs. 5.6 (a) and (b). In addition, the influence of the light leakage in this region is obscured due to the edge position.

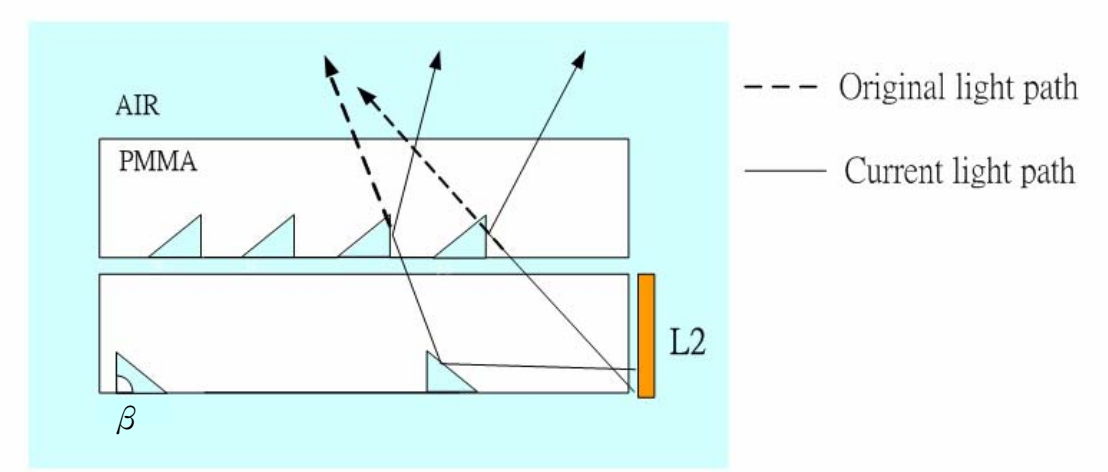

Fig. 5.7 Light paths for leaking to the opposite direction

On the other hand, the irregular vibrations of the angular distribution belong to the local properties, which are determined by the local groove structure and distribution. However, the influences of the groove structure are more critical because the proportion of the deviation to the designed groove parameters is much larger than that to the distribution parameters, i.e. about 25%, for the fabricated light-guide. The departures of the micro-groove structure include several parts: the inclined angle, the

right angle and the groove width, as shown in Fig. 5.3. If the groove angle was varied in a small range around the designed value, the peak width may be broadened without affecting the directionality. In addition, the variation of angle α at the micro-groove structure will not affect the angular distribution a lot because most light is totally reflected out on the inclined surface before the surface of right angle. But too large variation of α will result in more light leakage in the other direction. In other words, the major impact of the departures mentioned above is the vibrations of the luminance intensity, especially within the regions of crosstalk of less than 10%, as seen in the Figs. 5.5 and 5.6.

For the both light sources, the suitable angular distribution for 3D vision, i.e. crosstalk of less than 10%, is located between $\pm 8^\circ$ to $\pm 26^\circ$. Therefore, the corresponding suitable viewing distance is within 7 to 23 cm. As for the uniformity within the suitable viewing distance, it depends on the viewing position. The rapid drop beside the edges of the suitable angular distribution results in uniformity varies quickly in the edges of the viewing distance range. Fig. 5.8 shows the appearances of the dual directional backlight with a LC panel viewed at different angle. The uniformity in the middle of the viewing distance range is better and close to 70%.

The discussion above is focused on the dual directional backlight with a diffuser. Now we consider the situation when a LC panel is disposed on the backlight. Figs. 5.5 (f) and 5.6 (f) indicate the angular distribution of the backlight is not affected by the LC panel except the luminance intensity. After calculation, the transparent rate of the LC panel is about 6 to 7 %. However, the luminance is still higher than, or close to, 100 nits and bright enough for the mobile display.

Moiré` pattern occurs at the region where the pitch ratio of the color filter and the micro-groove pattern is close to 1 or 2 and can not be suppressed only by the diffuser, as seen in Fig. 5.8. Therefore, another design for free of the moiré` pattern, as

mentioned in chap 4, was further fabricated and presented below.

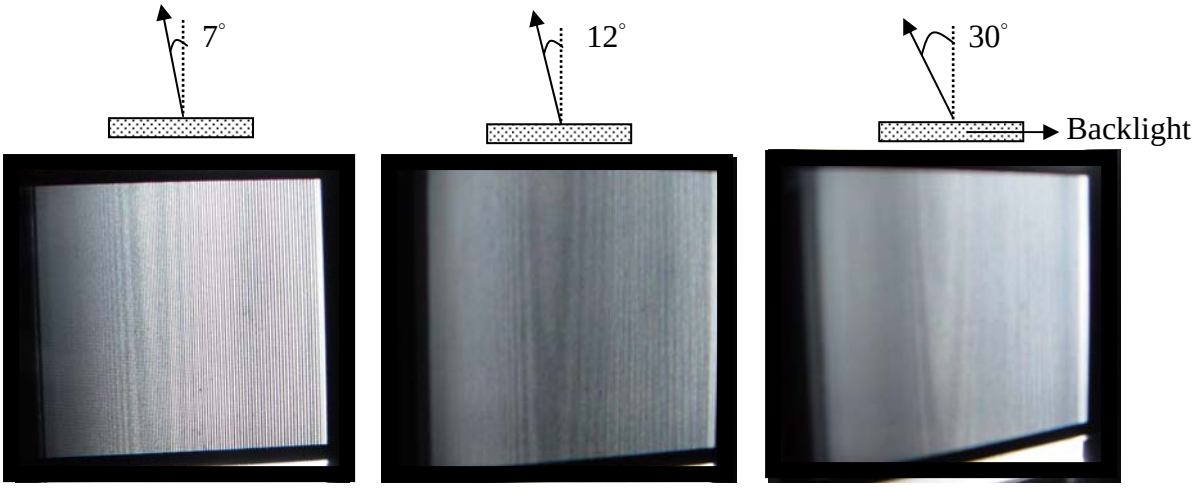

Fig. 5.8 Appearances of the backlight with a LC panel viewed at 7°, 12° and 30° respectively

5.4 Measured Results of the Dual directional Backlight with Partial Continuous Micro-groove Distribution

The dual directional backlight with partial continuous distribution was designed and fabricated to suppress the moiré` pattern. The fabricated micro-groove profiles and the optical performances of the dual directional backlight are shown and discussed in the following.

5.4.1 Micro-groove profiles

After improved the fabrication process, the fabricated micro-groove profiles are close to the desired groove shapes except the groove sizes. Fig. 5.9 shows the micro-groove profiles measured at different position, where the coordinate axis, y, is the same as that in simulation. The figures indicate the grove angle was regular in local area and departed from the designed value, 38°, in a smaller range, i.e. less than 3°. Besides, the variation of the right angle was also improved and negligible. On the other hand, the fabricated groove sizes still did not meet the designed values, which was contributed

to inadequate uniformities at some viewing directions and was discussed later.

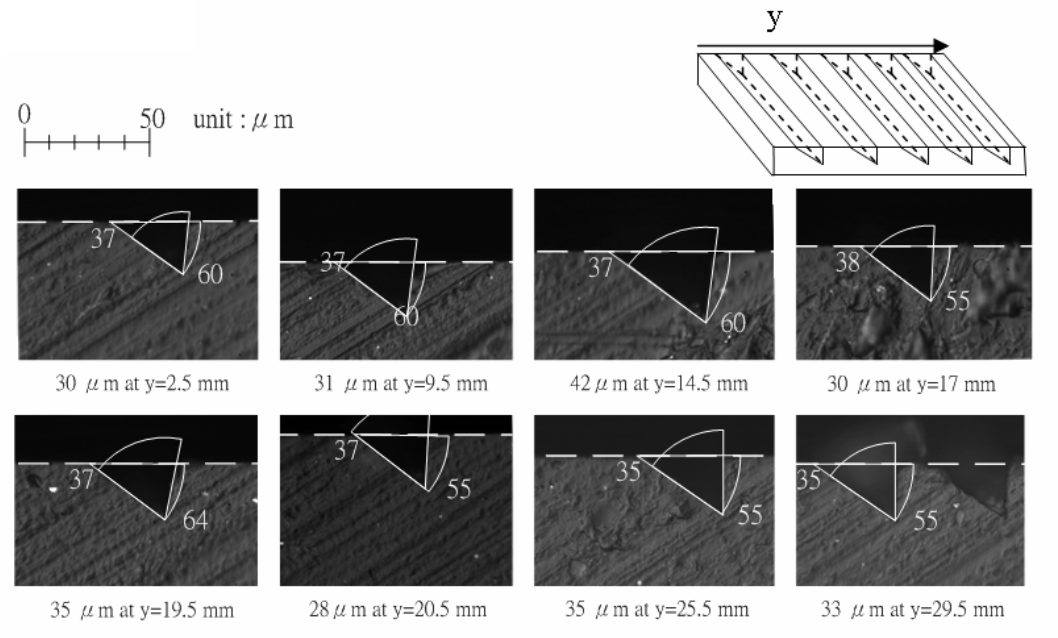

Fig. 5.9 Micro-groove profiles measured at different positions

5.4.2 Optical Performances

The optical performances of the dual directional backlight with partial continuous micro-groove distribution were further examined in this section. The optical appearances of the previous design and this design, both with a LC panel on the top, were presented at the same time in Fig. 5.10. In this figure, the moiré` pattern, produced by the color filter and the micro-groove pattern, was improved markedly by

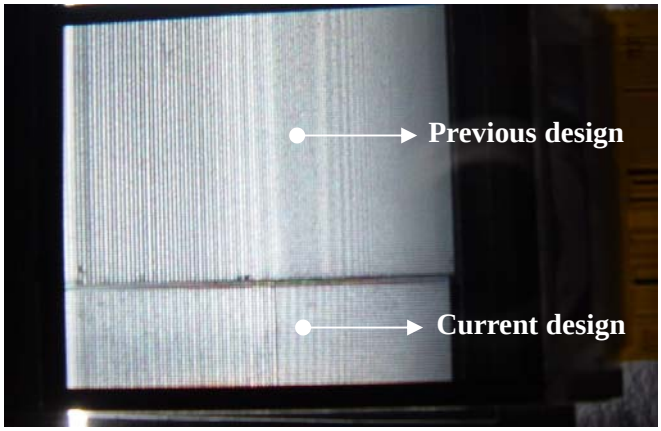

Fig. 5.10 Appearances of the previous design and current design with partial continuous micro-groove distribution, both with a LC panel on the top

the design with partial continuous micro-groove distribution, which gives the evidence for the validity of this design.

Similarly, the angular distributions at five different positions were measured and discussed as in the previous design. Figs. 5.11 and 5.12 show the angular distributions of the dual directional backlight for L1 and L2, respectively, where the corresponding regions with crosstalk of less than 10 % were also shown. Theses figures also behave similarly in some aspects, as mentioned in section 4.3.2, and the similar discussions are skipped here.

For the both light sources, the suitable angular distribution for 3D vision, i.e. crosstalk of less than 10%, is located between ±8° to ±40° and the corresponding suitable viewing distance is roughly within 4 to 23 cm. As for the uniformity within the suitable viewing distance, it also depends on the viewing position. Fig. 5.13 shows the appearances of the backlight with a LC panel viewed at 10°, 20° and 50°, respectively. The best uniformity is located around 15° and close to 75% while the uniformities viewed at other directions were inadequate due to the deviations of groove width.

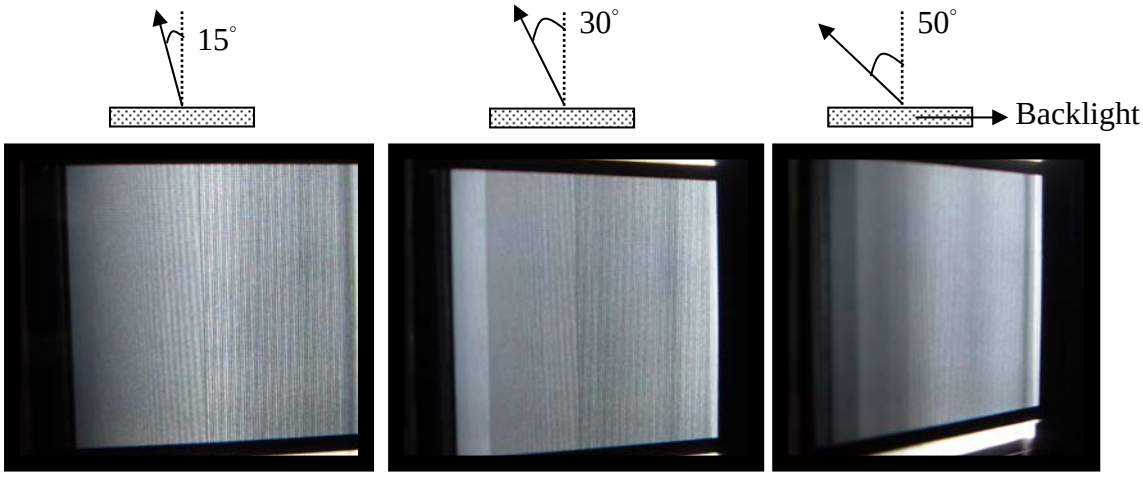

Fig. 5.13 Appearances of the backlight with a LC panel viewed at 15°, 30° and 50° respectively

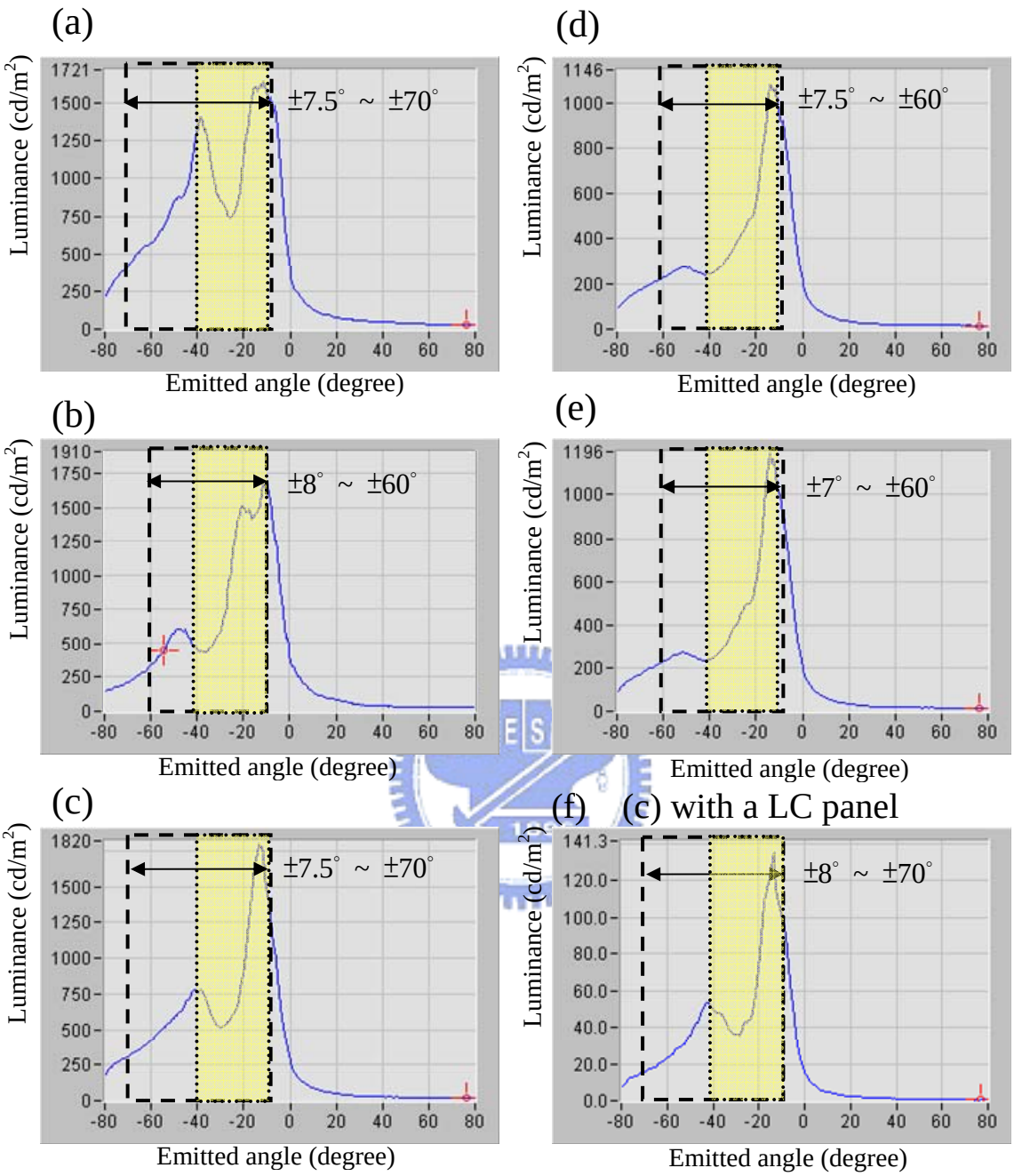

Fig. 5.13 Angular distributions of L1 measured at different positions on backlight: (a) above left, (b) below left, (c) center, (d) above right, (e) below right, and (f) (c) with LC panel. Crosstalk of less than 10% is located in the region marked by broken line. Suitable angular distribution for 3D vision, ±8° to ±40°, is marked by dotted line.

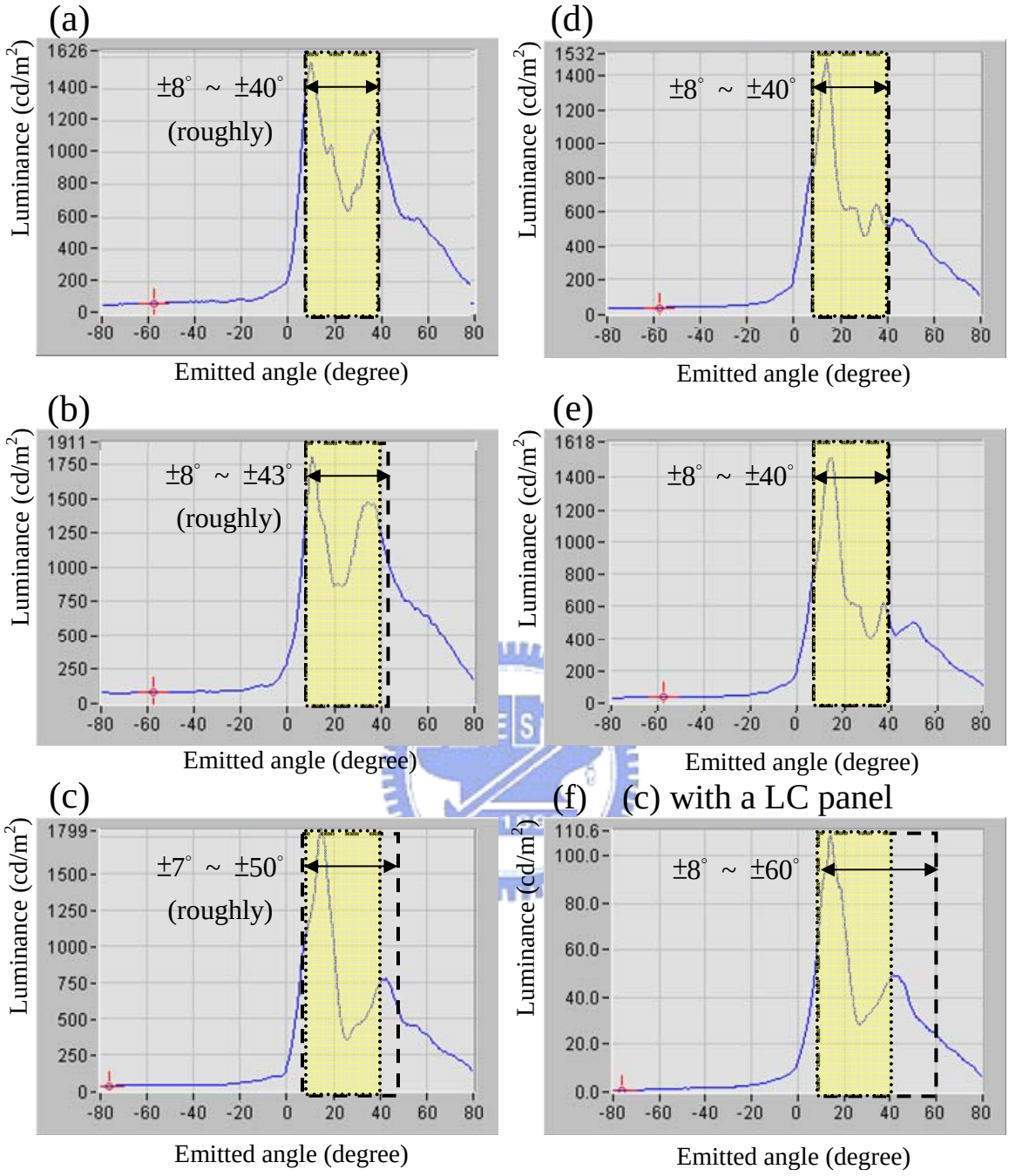

Fig. 5.14 Angular distributions of L2 measured at different positions on backlight: (a) above left, (b) below left, (c) center, (d) above right, (e) below right, and (f) (c) with LC panel. Crosstalk of less than 10% is located in the region marked by broken line. Suitable angular distribution for 3D vision, ±8° to ±40°, is marked by dashed line.

5.5 Summary

The measured angular distributions verify the distinguished directionalities of the fabricated directional light-guides, where the light leakage amount was controlled in a designed range by simple structures. For the dual directional backlight with continuous micro-groove distribution, the corresponding suitable viewing distance ranges for 3D vision is within 7 cm to 23 cm. Such viewing distance range may be shorter than the conventional viewing range for 2D version but especially suitable for better 3D vision on a small panel due to the larger parallax. On the other hand, the best uniformities of the design are close to 70%, while the uniformities viewed at other directions were inadequate due to the deviations of the groove structures. After some improvements, the optical performances of the dual directional backlight with partial continuous micro-groove distribution, for free of moiré` pattern, were better than that with continuous micro-groove distribution. In addition to the insensible moiré` pattern, the suitable viewing distance ranges for 3D vision is wider, i.e. within 4 cm to 23 cm. Besides, the best uniformities of the design are close to 75% while the uniformities viewed at other directions were still inadequate due to the deviations of the groove structures, which also can be further improved by the proper fabrication processes.

Chapter 6

Applcations

The applications of the proposed dual directional backlight and the requirements of the accompanying LC panel are described in this chapter. Furthermore, the cooperation status with an industrial collaborator for 3D mobile display will also be presented in the end.

The major applications of the dual directional backlight combined with a fast switch LC panel is to present two images at two certain directions for only one viewer or two viewers at different positions. For one viewer, 2D and 3D visions can be switched by projecting the same images or pairs of parallax images to the viewer` s eyes respectively. For two viewers at different positions, different image information can be viewed at different positions at the same time, without an extra display device. Similar applications have been carried out and some of them are shown in Fig. 6.1.

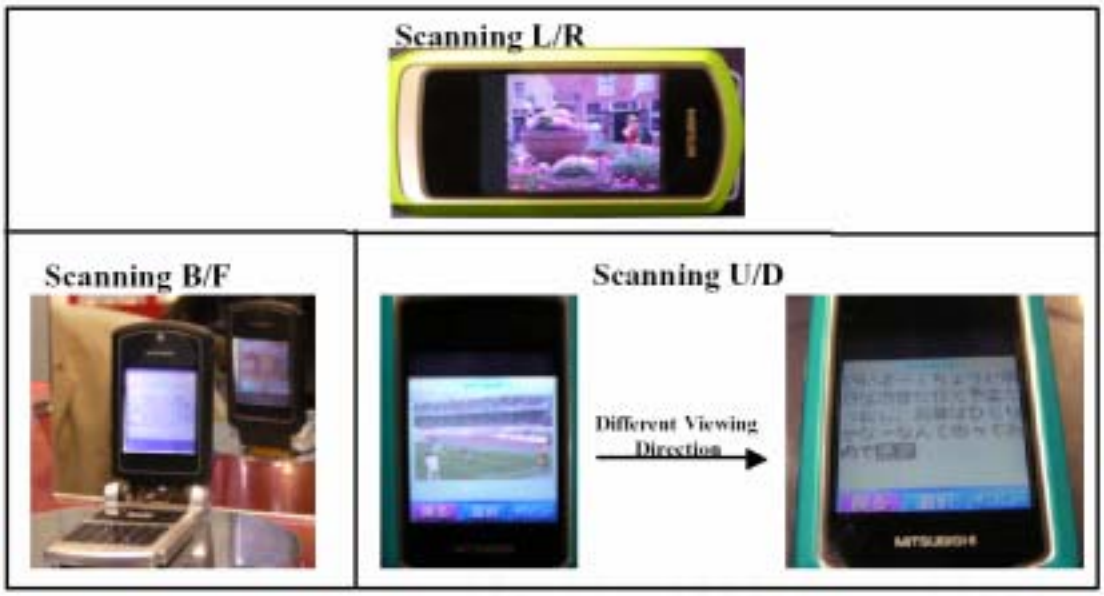

Fig. 6.1 Applications of the dual directional backlight (Mitsubishi, FPD 2004 exhibition)

In order to accomplish the applications mentioned above, a LC panel with fast response time is required. The critical fusion frequency (CFF) at which flicker becomes undetectable to the human eye is about 60 Hz [30]. To eliminate flicker, the field frequency of the time-multiplexed 3D display needs to set at about 120Hz, double the CFF. In other words, the response time of the LC shall be of less than 8 ms, which can be achieved by OCB (optically compensated bend) type [31] or ultra-thin TN (twisted nematric) LC panel currently.

In order to demonstrate the 3D mobile display with the dual directional backlight proposed here, we have cooperated with AU Optronics Corp., which supplies the related display technology, such as LC panels with fast response time and image driving. Now, A LC panel with response time of 7.1 ms has been achieved by over driving the 90° TN LC panel with cell gap of 2 μm, as shown in Fig. 6.2. But the response time for other grey scale is larger and may not fast enough. On the other hand, the current driving scheme, of equal writing time for each gate line, results in a pair of parallax images displayed at the same time, as shown in Fig. 6.3. To prevent projecting left-eye and right-eye image information to the same eye, a few common solutions are described below.

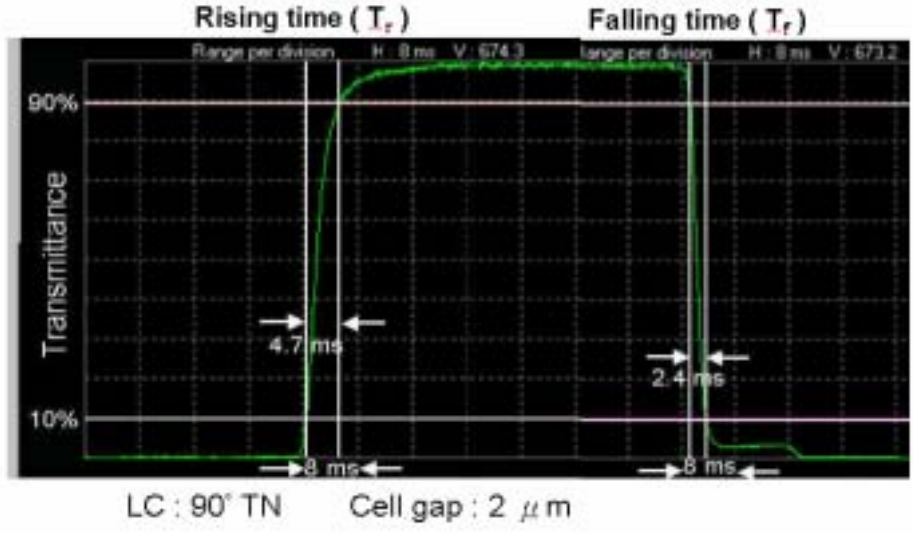

Fig. 6.2 Response time of TN LC (~7.1 ms)

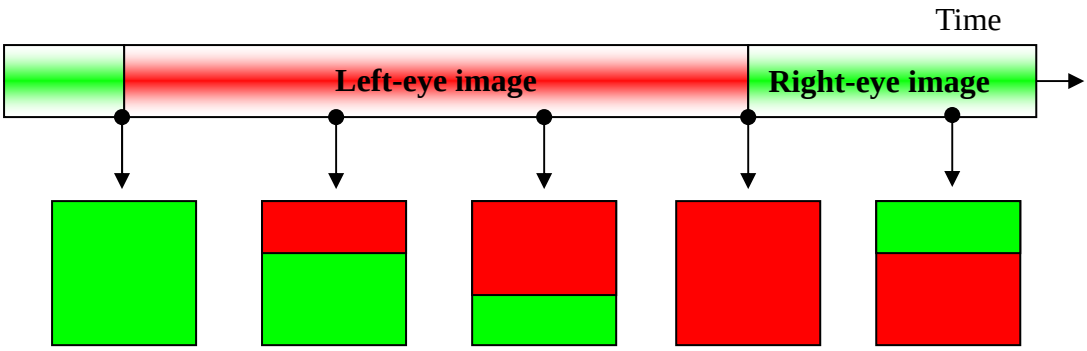

Fig. 6.2 Driving scheme of equal writing time for each gate line

The first solution is to change the driving scheme, where each gate line is scanned as fast as possible. Besides, each light source is off until the image is completely refreshed. Thus, the mixed image information will not be seen and cause crosstalk. The second solution is to insert a black frame between each image. However, this solution doubles the field frequency and requires an LC panel with fast response time of less than 4 ms, which is not feasible now. The third solution is to utilize scanning light sources. Ideally, only correct images are provided light source and projected to the designated eye. Now, all the solutions are still being investigated for feasibility and will be developed in the near future.

Chapter 7

Conclusions

With the expending demands for more attractive and natural viewing experiences, 3D display is expected to be the next key display technology and shall play an important role in the future. Among various 3D methods, such as stereoscopic, volumetric, holographic and stereo pair types, the stereo pair type is the most popular method due to the high compatibility with current 2D display and advantages of compact sizes and low cost. Particularly, the time-multiplexed stereo pair type has inherent advantages of no needs to sacrifice spatial qualities for displaying different image information and no alignment issue between the displayed images and the viewing zone forming optics. In the past few years, several directional backlights designed for 3D displays, based on time-multiplexed stereo pair type, have been proposed. However, they suffer from complex structures and alignment issue between each light-controlled pattern. In order to resolve the concerns mentioned above, a directional backlight system for 3D mobile display based on the time-multiplexed method was proposed in this thesis. The dual directional backlight system features only one simple micro-groove structure to control the light direction and, thus, no alignment issues occur.

The dual directional backlight consists of two identical light-guides, two light sources and a bottom absorber. Each light-guide with one surface patterned with micro-groove structures has a light-controlled ability of one direction. By fast switching the light sources, pairs of parallax images are directed to the viewer` s respective eyes sequentially. All properties of our design mentioned above should be characterized, therefore, a preliminary embodiment was designed and fabricated to

confirm the light-controlled ability. The designed light-guides were fabricated by diamond turning for the convenience and low cost. Finally, the measurement instruments were utilized to characterize the properties of the fabricated devices.

In simulation, we designed and optimized the dual directional backlight by varying micro-groove structures and distribution, including groove angle, groove width and gap. One of the optimized dual directional backlight with the specifications of groove angle of 38°, groove width of 25 μm and groove gap range between 25 and 368 μm was chosen. Furthermore, another dual directional backlight for free of moire` pattern was also designed and optimized, whose optimized specifications are groove angle of 38°, groove width varying from 18 to 27 μm and groove gap varying from 4 to 160 μm and varying from 270 to 290 μm in different part.

After fabricated by diamond turning, an optical microscope and an optical measurement system, Conoscope, were utilized to measure the fabricated micro-groove profiles on the directional light-guide and the angular distribution of the dual directional backlight, respectively. The crosstalk of less 10% for the dual directional backlight and that for free of moiré` pattern were located between ±8° to ±26° and ±8° to ±40°, respectively, where the corresponding viewing distance, suitable for 3D vision, were roughly within 7 to 23 cm and 4 to 23 cm, respectively. Such viewing distance range may be shorter than the conventional viewing range for 2D version but especially suitable for better 3D vision on a small panel due to the larger parallax. On the other hand, the best uniformity of the dual directional backlight was close to 70% while the uniformities viewed at other directions were inadequate due to the deviations of the groove structures. After improved the fabrication process, the best uniformity of the dual directional backlight for free of moiré` pattern was close to 75% but the uniformities viewed at other directions were still inadequate due to the deviations of the groove structures. However, uniformity

can be further improved by the proper fabrication process.

From the experimental results, the light-controlled ability of the dual directional backlight was verified. Besides, the luminance of the dual directional backlight with a LC panel on the top was higher than 100 nits and high enough for a small panel. In spite of the inadequate uniformity caused by the fabrication deviations, we can say that the proposed dual directional backlight provides time-multiplexed 3D display with adequate directionalities and light efficiency by utilizing much simpler structure.

In the future, in addition to improving the optical performances of the dual directional backlight by improving the fabrication process, a complete 3D mobile display can be realized by combining the dual directional backlight with a fast switching liquid crystal display with response time of less than 8ms. Currently, an industrial collaborator is fabricating the fast switching LCDs and image driving. Now a LC panel with response time of 7.1 ms has been achieved by over driving the 90° TN liquid crystal panel with cell gap of 2 μm. Besides, a few solutions to image driving are under investigation for feasibility and will be developed in the near future.

Reference

[1] J. A. Castellano, *Hanbook of display technology*, Chapter 1, Academic Press, Inc., San Diego (1992).

[2] T. Ito, *Foundations of the 3D television*, NHK Sci. & Tech. Res. Labs., p.93, Ohmsha, Ltd, Tokyo (1995).

[3] B. Javidi and F. Okano, *Three-Dimensional Television, Video, and Display Technologies*, p.4, Springer (2002).

[4] T. Ito, *Foundations of the 3D television*, NHK Sci. & Tech. Res. Labs., p.13, Ohmsha, Ltd, Tokyo (1995).

[5] G. R. Ogram, *Magical Images*, Chapter 5 (2001).

[6] B. Lane, Stereoscopic displays proceedings of the SPI*E*, Vol. 0367 (1982).

[7] T. Ito, *Foundations of the 3D television*, NHK Sci. & Tech. Res. Labs., Ohmsha, Ltd, Tokyo, p.135 (1995).

[8] B. Javidi and F. Okano, *Three-Dimensional Television, Video, and Display Technologies*, Springer, p.35 (2002).

[9] G. E. Favalora, R. K. Dorval, D. M. Hall, M. G. Giovinco, J. Napoli, *Volumetric 3D display system with rasterization hardware*, Stereoscopic Displays and Virtual Reality Systems VIII, Proc. SPIE Vol. 4297, p. 227 (2001).

[10] A. Sullivan, *"A Solid-state Multi-planar Volumetric Display"*, SID"03, p.1531 (2003).

[11] H. Takada, S. Suyama, K. Hiruma, and K. Nakazawa," *A Compact Depth-Fused 3-D LCD*", SID"03, p.1526 (2003).

[12] G. K. Starkweather, "*DSHARP –A Wide Screen Multi-projector Display*", SID"03, p.1535 (2003).

[13] P. St.-Hilaire, S.A. Benton, M. Lucente, and P. M. Hubel, *"Color Images with the*

MIT Holographic Video Display", Practical Holography VI, Proc. SPIE Vol. 1667, p.73 (1992).

[14] D. J. Sandin, et al.," *Computer-generated Barrier-stripe Autostereography"*, Proc. SPIE, p.1083 (1989).

[15] H. Isono, M. Yasuda, and H. Sasazawa, "Autostereoscopic 3D LCD Display Using LCD-generated Parallax Barrier," in *Proc. 12th Int. Display Research Conf. '92*, Tokyo, Japan, p.303 (1992).

[16] H. Morishama, H. Nose, N. Taniguchi, K. Inoguchi, S. Matsumura, "An Eyeglass-Free Rear-Cross-Lenticular 3D Display", SID Intl Symp Tech Papers, p.923-926 (1998)

[17] S. Ichinose, et al.," *Full-color Stereoscopic Video Pickup and Display Technique without Special Glasses*", Proc. SID"89, p.319 (1989).

[18] B. Javidi and F. Okano, *Three-Dimensional Television, Video, and Display Technologies*, Springer, p.36 (2002).

[19] Y. Kim, et al. "*Viewing-Angle-Enhanced 3-D Integral Imaging System Using a Curved Lens Array*", SID'04, p.1442 (2004).

[20] B. Lee, S. Y. Jung, J. H. Park, "*Three-dimensional Integral Imaging Using LCD and LC Polarization Switcher*", Asian Symposium on Information Display, p.109 (2004).

[21] K. Toyooka, T. Miyashita and T. Uchida, "*The 3D Display Using Field-Sequential LCD with Light Direction Controlling Back-light*", SID'01, p.174 (2001).

[22] T. Sasagawa, A. Yuuki, S. Tahata, O. Murakami, and K. Oda," *Dual Directional Backlight for Stereoscopic LCD*", SID'03, p.399 (2003).

[23] K. W. Chien and H. P. D. Shieh, "*Time-multiplexed 3D Displays based on Directional Backlights with Fast Switching Liquid Crystal Displays*", Appl. Opt.

accepted.

[24] E. Hecht, *Optics* (3rd version), Addison Wesley Longman Inc., p.119 (1998)

[25] C. Y. Tasi: Master thesis, National Chiao-Tung University, Taiwan, June 1999.

[26] H. Yang, *Introduction of Precision Micromachining Technology*, CHWA , p.1-9 (2004).

[27] H. Yang, *Introduction of Precision Micromachining Technology*, CHWA, p.5-2 (2004).

[28] B. P. John, *Scaling Down of Manufacturing Systems: Meso and Nano Level Machining – An Analysis*, PSU, p.6 (2003).

[29] Y. Yeh, and L. Silverstein, "*Human Factors for Stereoscopic Color Displays*", SID'91 Digest, p.826 (1991).

[30] H. Imai, S. Tsujikawa, M. Imai, NEC Corp.," *Viewing Point Detection System Using Specific Image Processing for Eye Position Tracking Autostereoscopic Display* ", Proc. SPIE V. 3639, p.92 (1999)

[31] K. Toyooka, T. Miyashita and T. Uchida, "*The 3D Display Using field-Sequential LCD with Light Direction Controlling Back-light*", SID'01, p.174 (2001)